



1 **Assessing the influence of water sampling strategy on the performance of tracer-**
2 **aided hydrological modeling in a mountainous basin on the Tibetan Plateau**

3 Yi Nan¹, Zhihua He², Fuqiang Tian¹, Zhongwang Wei³, Lide Tian⁴

4 ¹ Department of Hydraulic Engineering, State Key Laboratory of Hydroscience and Engineering,
5 Tsinghua University, Beijing, China

6 ² Center for Hydrology, University of Saskatchewan, Saskatchewan, Canada

7 ³ Guangdong Province Key Laboratory for Climate Change and Natural Disaster Studies, School of
8 Atmospheric Sciences, Sun Yat-sen University, Guangzhou, Guangdong, China

9 ⁴ Institute of International Rivers and Eco-security, Yunnan University, Kunming, China

10 **Corresponding to:** Fuqiang Tian

11 Email: tianfq@tsinghua.edu.cn

12



13 **Abstract**

14 Tracer-aided hydrological models integrating water isotope module into the simulation of
15 runoff generation are useful tools to reduce uncertainty of hydrological modeling in cold basins
16 that are featured by complex runoff processes and multiple runoff components. However, there
17 is little guidance on the strategy of field water sampling for isotope analysis to run tracer-aided
18 hydrological models, which is especially important for large mountainous basins on the Tibetan
19 Plateau (TP) where field water sampling work is highly costly. This study conducted a set of
20 numerical experiments based on the THREW-1 model to evaluate the reliance of the tracer-
21 aided modeling performance on the availability of site measurements of water isotope in the
22 Yarlung Tsangpo River (YTR) basin on the TP. Data conditions considered in the numerical
23 experiments included the availability of glacier meltwater isotope measurement, quantity of site
24 measurements of precipitation isotope, and the variable collecting strategies for stream water
25 sample. Our results suggested that: (1) In high-mountain basins where glacier meltwater
26 samples for isotope analysis are not available, estimating glacier meltwater isotope by an offset
27 parameter from the precipitation isotope is a feasible way to force the tracer-aided hydrological
28 model. Using a set of glacier meltwater $\delta^{18}\text{O}$ that were 2‰~9‰ lower than the mean
29 precipitation $\delta^{18}\text{O}$ resulted in only small changes in the model performance and the
30 quantifications of contributions of runoff components (CRCs, smaller than 5%) to streamflow
31 in the YTR basin; (2) strategy of field sampling for site precipitation to correct the global
32 gridded isotope product of isoGSM for model forcing should be carefully designed. Collecting
33 precipitation samples at sites falling in the same altitude tends to be worse at representing the
34 ground pattern of precipitation $\delta^{18}\text{O}$ over the basin than collecting precipitation samples from
35 sites in a range of altitudes; (3) Collecting weekly stream water samples at multiple sites in the
36 wet and warm seasons is the optimal strategy for calibrating and evaluating a tracer-aided
37 hydrological model in the YTR basin. It is highly recommended to increase the number of
38 stream water sampling sites rather than spending resource on extensive sampling of stream
39 water at a sole site for multiple years. These results provide important implications for
40 collecting site measurements of water isotope for running tracer-aided hydrological models to
41 improve quantifications of CRCs in the high-mountain basins.

42



43 1. Introduction

44 Catchments located in mountainous regions generally provide important water resources
45 for downstream regions (Viviroli et al., 2003). As typical mountainous cryosphere, TP is the
46 source region for several large rivers in Asia, and has been called 'water tower' because of
47 its importance for downstream livelihoods and agricultural irrigations (Schaner et al., 2012).
48 Dominant characteristic of mountainous catchments on TP is the multiphase of water sources
49 that generate runoff and the consequently complex hydrological processes, highlighting the
50 importance of accurately quantifying the contributions of runoff components (CRCs) to
51 streamflow for better understanding the runoff dynamics under changing climate. This task
52 is difficult due to the complex hydrological processes being insufficiently represented by
53 typical hydrological models, leading to large uncertainty of hydrological simulations (He et al.,
54 2018). Due to the strong inter-compe^{sat}ion of runoff processes induced by different water
55 sources and runoff pathways (Duethmann et al., 2015), uncertainties of the modeled CRCs in
56 mountainous basins on the TP are rather high. Utilizing more datasets to evaluate the model
57 performance is a feasible way to constrain modeling uncertainty and improve quantifications
58 of CRCs in cold regions (Chen et al., 2017).

59 Tracer-aided hydrological models integrating environmental tracer (e.g., stable oxygen
60 isotope, ^{18}O) modules into runoff generation processes have proved helpful for parameter
61 calibration, model structure diagnosis and CRC quantification (Son and Sivapalan, 2007; Birkel
62 et al., 2011), and are increasingly adopted in cold catchments (e.g., Ala-aho et al., 2017; He et
63 al., 2019; Nan et al., 2021a). Recent research^{res} indicated that estimates of precipitation $\delta^{18}\text{O}$
64 from outputs of isotopic general circulation models (iGCMs) perform well on forcing tracer-
65 aided models in large basins with a low cos^{of} water sampling (Delavau et al., 2017; Nan et al.
66 2021b). Similarly to the tracer-based end-member mixing methods that utilize the different
67 tracer signatures of water sources to separate the hydrograph and quantify CRCs (Klaus and
68 McDonnell, 2013; He et al., 2020), the tracer-aided hydrological models used the differed
69 isotopic compositions of runoff components to co^{sur} in the water apportionments in runoff
70 generation. The isotopic compositions of runoff components strongly differ in high-mountain
71 basins resulting from the following two reasons: One is the significantly more depleted $\delta^{18}\text{O}$
72 of meltwater compared to that of rain, due to the altitude and temperature effects, and the
73 fractionation effect during melting processes (Xi, 2014; Boral and Sen, 2020). Another is the
74 damping and lagging isotopic variability of subsurface runoff pathway, compared to that of
75 surface runoff, as a result of the catchment hydrological functions of storing, mixing and
76 transporting water (Bowen et al., 2019; Birkel and Soulsby, 2015; McGuire and McDonnell,
77 2006). Consequently, water isotope signatures bear ^{zoo} potentials to improve the
78 representations of internal hydrological processes in hydrological models, if observations of
79 water isotopes were involved in the model calibration and evaluation procedures (McGuire et



80 al., 2007; He et al., 2019).

81 Although a plenty of isotope-based works have been conducted in mountainous
82 catchments on the TP to improve understandings of local hydrological processes (e.g., Li et al.,
83 2020; Kong et al., 2019; Tan et al., 2021), but they provided guidance on data collection of
84 water isotope for hydrological applications in large mountainous areas. Some water sampling
85 works in large mountainous catchments were conducted in a single field campaign (e.g., Xia et
86 al., 2019; Dong et al., 2018), which is, although helpful to understand the generations of short-
87 term runoff events, not suitable for the calibration of tracer-aided models in a multi-year
88 simulation period (Knapp et al., 2019; Zhang et al., 2019). An exception is Stevenson et al.
89 (2021) who utilized a 7-year dataset of stream water $\delta^{18}\text{O}$ in a 3.2 km² catchment to analyze the
90 effects of stream water sampling strategies on the calibration of a tracer-aided hydrological
91 model. Challenges arise when transferring their findings to the application of tracer-aided
92 hydrological models in large high-mountain basins: First, it is questionable that whether
93 sampling stream water at one site can adequately represent the isotope signature of stream water
94 over the whole basin, considering the strong spatial variability of hydrological processes caused
95 by the heterogeneity in meteorological factors and land surface conditions in mountains (Wang
96 et al., 2021; Li et al., 2020). Second, the influences of data collection of precipitation isotope
97 on the performance of tracer-aided hydrological models remain unclear. Results of He et al.
98 (2019) indicated that monthly sampling of precipitation at two sites seems to be able to capture
99 the isotope variations in a 233 km² catchment. However, the requirement of isotope data
100 quantity to adequately capture the spatial pattern of precipitation isotope signature for forcing
101 tracer-aided models in large basins ($\sim 10^5$ km²) is poorly explored (Nan et al., 2021b). Third, in
102 glacierized mountainous catchments where streamflow was fed by additional water source of
103 glacier melt, the requirement of glacier meltwater samples for the forcing and evaluation of
104 tracer-aided hydrological models is also unclear. Consequently, better understandings of how
105 water sampling strategies influence the value of water isotope data for aiding hydrological
106 modeling, is highly helpful for guiding the establishment of monitoring systems of water
107 isotope in large mountainous regions. Considering the high costs of human and financial
108 resources of collecting water samples in TP area, it is important to take efficient strategies for
109 water sampling that balance the trade-off between field work burden and data adequacy well
110 (Sprenger et al., 2019).

111 Motivated by the mentioned backgrounds, we conducted detailed analysis on the tracer-
112 aided model performance in a large mountainous basin on the TP under different assumed
113 situations with respect to the collection strategy of site water isotope data, based on a numerical
114 experiment method. We adopted the tracer-aided hydrological model THREW-T developed by
115 Nan et al. (2021a), which was forced by the global gridded isotope outputs of iGCM being
116 corrected by measurements of precipitation $\delta^{18}\text{O}$, to achieve the research aim. Three specific



117 questions were addressed: (1) how does the estimated isotopic composition of glacier meltwater
118 influence the performance of tracer-aided hydrological modeling when no glacier meltwater
119 samples were available, (2) how does the collection strategy of site precipitation samples for
120 the correction of iGCM influence the model performance, and (3) how does the sampling
121 strategy of stream water influence the model calibration and evaluation?

122 **2. Materials and methodology**

123 **2.1 Study area**

124 The Yarlung Tsangpo River (YTR) basin, located in the southern TP (Fig. 1), extends in
125 the ranges of 27°N -32°N and 82°E -97°E, with an elevation extent of 2900-6900 m above sea
126 level (a.s.l.), which is one of the largest basins on the TP. The mean annual precipitation in the
127 YTR basin is around 470mm featured by a distinct wet season from June to September, due to
128 the dominance of the South Asian monsoon. Drainage area above the Nuxia hydrological station
129 at the basin outlet is approximately 2×10^5 km², and around 2% of which is covered by glacier.

130 The Karuxung River (KR) catchment is located in the upper regions of the YTR basin, and
131 was chosen as a supplementary experiment catchment, because of the long term field work of
132 water sampling in this catchment. The KR originates from the Lejin Jangsan peak of the Karola
133 mountain (7206m a.s.l.), and flows into the Yamdrok Lake (4550m a.s.l.), draining an area of
134 around 286 km². Streamflow in the KR catchment is strongly influenced by glaciers which
135 cover an area of 58 km².

136 **[Figure 1]**

137 **2.2 Hydro-meteorological and water isotope data**

138 Elevation of the YTR basin was derived from a digital elevation model (DEM) with a
139 spatial resolution of 30m from the Geospatial Data Cloud (<https://www.gscloud.cn>). Daily
140 meteorological inputs including precipitation, temperature and potential evapotranspiration
141 were collected from the 0.1°×0.1° China Meteorological Forcing Dataset (CMFD, Yang and
142 He, 2019). The second glacier inventory data set of China (Liu, 2012) and the Tibetan Plateau
143 Snow Cover Extent product (TPSCE, Chen et al., 2018) were used to denote the glacier and
144 snow coverages. Vegetation coverages were extracted from the MODIS satellite products of
145 eight-day leaf area index (LAI) dataset MOD15A2H (Myneni et al., 2015) and monthly
146 normalized difference vegetation index (NDVI) dataset MOD13A3 (Didan et al., 2015). Soil
147 types and properties in the tested basins were collected from the Harmonized World Soil
148 Database (HWSD, He, 2019). Observations of daily streamflow during 2000-2015 at the Nuxia,
149 and that during 2000-2010 at Yangcun and Nugesha stations were used for hydrological model
150 evaluation.



151 In the KR catchment, daily temperature and precipitation during 2006-2012 were collected
 152 at the Langkazi meteorological station. Altitudinal distributions of temperature and
 153 precipitation across the KR catchment were estimated based on the lapse rates reported in
 154 Zhang et al. (2015). Daily streamflow during 2006-2012 was measured at the Wengguo
 155 hydrological station.

156 Outputs of the scripps global spectral model with water isotopes incorporated (isoGSM,
 157 Yoshimura et al., 2008) with the spatial and temporal resolutions of $1.875^\circ \times 1.875^\circ$ and 6h were
 158 extracted to represent the spatio-temporal pattern of the precipitation isotope in the YTRbasin.
 159 According to our previous evaluation of the isoGSM product, it overestimated precipitation
 160 $\delta^{18}\text{O}$ in the YTR basin (Nan et al., 2021b). To correct bias in the isoGSM products, grab samples
 161 of precipitation were collected in the wet season of 2005 at four stations along the main channel
 162 of YTR, i.e., Nuxia (3691 m a.s.l.), Yangcun (4541m a.s.l.), Nugesha (4715m a.s.l.) and Lazi
 163 (4889m a.s.l.). The precipitation water samples were collected as soon as possible after the
 164 precipitation event in order to avoid the effect of evaporation. Stream water samples were
 165 collected weekly during the same period from river at the four stations.

166 The isoGSM isotope products were corrected by Eqs. 1-3: First, the bias of isoGSM
 167 product was assumed to be linearly related to altitude. Relation between the mean bias of
 168 isoGSM products and altitude was estimated by a least square method using $\delta^{18}\text{O}$ measurements
 169 of precipitation samples and gridded isoGSM estimates at the four sampling sites (Eqs. 1-2);
 170 Second, on each grid of the isoGSM product, isoGSM estimate was corrected by a bias
 171 estimated by the grid altitude in Eq. 3 based on the availability of $\delta^{18}\text{O}$ measurements from
 172 precipitation site samples on the date.

$$173 \quad B_i = \overline{\delta^{18}O_{i,M}} - \overline{\delta^{18}O_{i,G}} \quad (1)$$

$$174 \quad B = a \cdot H + b \quad (2)$$

$$175 \quad \delta^{18}O_{k,j,\text{Corr}} = \begin{cases} \delta^{18}O_{k,j,G} + B_k, & \text{for date } j \text{ with no data} \\ \frac{\sum_{i=1}^4 \delta^{18}O_{i,j,M} - \frac{\sum_{i=1}^4 \overline{\delta^{18}O_{i,M}}}{4} + \overline{\delta^{18}O_{k,G}} + B_k}{4} & \text{for date } j \text{ with data} \end{cases} \quad (3)$$

176 where, B_i is the bias of isoGSM at sites i . $\overline{\delta^{18}O_{i,M}}$ and $\overline{\delta^{18}O_{i,G}}$ are the weighted average of the
 177 site measurement and isoGSM estimate over the sampling period at sites i , respectively. H is
 178 the altitude of the sampling site. Parameters a and b are the linear regression coefficients, which
 179 were estimated as -0.0046 and 14.96 by the least square method in this study. $\delta^{18}O_{k,j,\text{Corr}}$
 180 is the corrected isoGSM precipitation isotope, and $\delta^{18}O_{k,j,G}$ refers to the original isoGSM
 181 isotope estimate at the hydrological model unit k on the date j .

182 Glacier meltwater $\delta^{18}\text{O}$ was assumed to be constantly lower than the weighted average of
 183 precipitation $\delta^{18}\text{O}$ by an offset parameter (Δ_δ) during the study period (Eq. 4) because of the
 184 unavailability of glacier meltwater samples, which is generally within the range of 2-9‰ in the



185 worldwide mountain regions (Rai et al., 2019; Wang et al., 2016; He et al., 2019; Ohlanders et
186 al., 2013; Jeelani et al., 2017) and is adopted as 5‰ from Boral and Sen (2020) in the YTR
187 basin.

$$188 \quad \delta^{18}O_{k,GM} = \overline{\delta^{18}O_{k,Corr}} - \Delta\delta \quad (4)$$

189 In the KR catchment, grab samples of precipitation and stream water were collected at the
190 Wengguo station in 2006-2007 and 2010-2012 for isotope analysis. The spatial distribution of
191 precipitation $\delta^{18}O$ was estimated based on an altitudinal lapse of -0.34‰/100 as reported in Liu
192 et al. (2007). Glacier meltwater $\delta^{18}O$ was assumed to be constant at -18.9‰ during the study
193 period (similarly to Gao et al. 2009). Details of precipitation and stream water samples in the
194 YTR and KR catchments were summarized in Table 1.

195 [Table 1]

196 2.3 Tracer-aided hydrological model

197 A distributed tracer-aided hydrological model, THREW-T (Tsinghua Representative
198 Elementary Watershed - Tracer-aided version) model developed by Tian et al. (2006) and Nan
199 et al. (2021a) was adopted for streamflow and isotope simulations. This model uses the
200 representative elementary watershed (REW) method for spatial discretization of catchment
201 (Reggiani et al., 1999). The study catchment is first divided into REWs based on DEM, and
202 each REW is further divided into two vertical layers (surface and subsurface layers), including
203 eight hydrological subzones based on the land cover and soil properties. In total, 63 41
204 REWs were extracted for the YTR basin and KR catchment, respectively (Tian et al., 2020;
205 Nan et al., 2021a, 2021b). Areal averages of the gridded estimates of meteorological variables,
206 vegetation cover and soil property were calculated in each REW to drive the model. A module
207 representing glacier melting and snowpack evolution was incorporated into the model for
208 application in cold regions (He et al., 2015; Xu et al., 2019; Tian et al., 2020). The tracer-aided
209 module was developed by Nan et al. (2021a), which simulated the isotope mixing and
210 fractionation processes based on complete mixing assumption and Rayleigh fractionation
211 method (similarly to He et al. 2019; Hindshaw et al., 2011; Wolfe et al., 2007). Forced by the
212 inputs of precipitation and glacier meltwater isotopic compositions, the model simulates the
213 isotope evolution in all the water sources in the watershed, including stream water, soil water
214 and snowpack. The iGCM isotope products properly corrected by $\delta^{18}O$ measurements of
215 precipitation samples have proved feasible to force the THREW-T model in large catchments
216 like YTR on the TP (Nan et al., 2021b).

217 The THREW-T model quantified the contributions of runoff components (CRC) to
218 streamflow based on two definitions of runoff components as reviewed in He et al. (2021). The
219 first definition is based on the individual water sources in the total water input triggering runoff



220 processes, including rainfall, snowmelt and glacier melt. The second definition is based on
 221 pathways of runoff-generation processes, resulting in surface and subsurface runoff (baseflow).
 222 More details of the model description and setup are given in Tian et al. (2006) and Nan et al.
 223 (2021a).

224 Physical basis and value ranges of the calibrated parameters in the THREW-T model were
 225 described in Table 2. Two kinds of calibration approaches were conducted: (1) a bi-objective
 226 calibration using discharge and SCA, and (2) a tri-objective calibration using discharge, SCA
 227 and stream water $\delta^{18}\text{O}$. Metrics used to evaluate the model performance are listed in Eqs. 5-8.
 228 The Nash-Sutcliffe efficiency coefficient (NSE) was used to optimize the simulation of
 229 discharge and isotope, whereas the root-mean-square error (RMSE) was used for the evaluation
 230 of SCA simulation. The Logarithmic Nash-Sutcliffe efficiency coefficient (lnNSE) was used
 231 additionally for discharge calibration to assess the simulation of baseflow. The model
 232 parameters were calibrated by streamflow and SCA observations during 2001-2010 (at Nuxia
 233 station) and 2006-2012 in the YTR and KR basins, respectively. The model performance in
 234 YTR basin was evaluated by the Nuxia streamflow and SCA observations during 2011-2015,
 235 and the streamflow observations at Yangcun and Nugesha stations during 2001-2010.

$$236 \quad \text{NSE}_{\text{dis}} = 1 - \frac{\sum_{i=1}^n (Q_{o,i} - Q_{s,i})^2}{\sum_{i=1}^n (Q_{o,i} - \bar{Q}_o)^2} \quad (5)$$

$$237 \quad \text{NSE}_{\text{Indis}} = 1 - \frac{\sum_{i=1}^n (\ln Q_{o,i} - \ln Q_{s,i})^2}{\sum_{i=1}^n (\ln Q_{o,i} - \ln \bar{Q}_o)^2} \quad (6)$$

$$238 \quad \text{RMSE}_{\text{SCA}} = \sqrt{\frac{\sum_{i=1}^n (\text{SCA}_{o,i} - \text{SCA}_{s,i})^2}{n}} \quad (7)$$

$$239 \quad \text{NSE}_{\text{iso}} = 1 - \frac{\sum_{i=1}^n (\delta^{18}\text{O}_{o,i} - \delta^{18}\text{O}_{s,i})^2}{\sum_{i=1}^n (\delta^{18}\text{O}_{o,i} - \bar{\delta^{18}\text{O}_o})^2} \quad (8)$$

240 where, n is the total number of observations. Subscripts of “o” and “s” refer to observed and
 241 simulated variables, respectively.

242 An automatic algorithm Python Surrogate Optimization Toolbox (pySOT) developed by
 243 Eriksson et al. (2017) was adopted for the multiple-objective optimization. The pySOT
 244 algorithm used a surrogate model to guide the search for improved solutions, with the advantage
 245 of needing few function evaluations to find a good solution. In each pySOT running, the
 246 optimization procedure was stopped if a maximum number of allowed function evaluations was
 247 reached, which was set as 3000 in this study. For the bi- and tri-objective calibrations,
 248 $0.5 \cdot (\text{NSE}_{\text{dis}} + \text{NSE}_{\text{Indis}}) - \text{RMSE}_{\text{SCA}}$ and $0.5 \cdot (\text{NSE}_{\text{dis}} + \text{NSE}_{\text{Indis}}) - \text{RMSE}_{\text{SCA}} + \text{NSE}_{\text{iso}}$ were chosen as
 249 the combined optimization objectives. For each scenario, the pySOT algorithm was repeated
 250 100 times, and behavioral parameter sets were selected among the 100 final results according
 251 to the performance metric thresholds, i.e., only the parameter sets producing metrics better than
 252 certain threshold values were regarded as behavioral parameter sets. The threshold values of
 253 evaluation metrics were used as $0.5 \cdot (\text{NSE}_{\text{dis}} + \text{NSE}_{\text{Indis}}) > 0.8$, $\text{RMSE}_{\text{SCA}} < 0.08$ in the YTR basin;



254 and $NSE_{dis} > 0.7$, $RMSE_{SCA} < 0.15$ in the KR catchment.

255 [Table 2]

256 2.4 Numerical experiments

257 [Table 3]

258 *Experiment 1: influence of assumed glacier meltwater isotope*

259 The first experiment was designed to test the reliance of model performance on the
260 assumed glacier meltwater isotope, as glacier melt water samples are typically not available for
261 isotope analysis in high mountain basins on the TP. In this experiment, variable glacier melt
262 isotope signatures were used to force the model, assuming the glacier meltwater $\delta^{18}O$ is 1‰,
263 3‰, 7‰ and 9‰ (i.e., Δ_{δ} values in Table 3) lower than the long-term average $\delta^{18}O$ of
264 precipitation. A benchmark model running by the literature based Δ_{δ} value of 5‰ was used as
265 a baseline reference to assess the influence of the assumed glacier meltwater isotope on the
266 model performance.

267 *Experiment 2: influence of site measurement of precipitation isotope*

268 The second experiment was designed to test the reliance of the model performance on the
269 availability of measured site precipitation isotope that was used to correct the isoGSM product.
270 The benchmark model running was forced by corrected isoGSM based on measurements of
271 precipitation isotope from all the four sampling sites (Figure 1). Three scenarios regarding the
272 availability of measured precipitation isotope were designed as shown in Table 3. First, we
273 assumed that only precipitation isotope measured at the two downstream sites of Nuxia and
274 Yangcun are available for the correction of isoGSM (i.e., scenario P_2stationNY in Table 3).
275 Second, we assumed that precipitation isotope measurement at the most upstream site Lazi is
276 available in addition to the measurement at the downstream site Nuxia (i.e., scenario
277 P_2stationNL in Table 3). Third, we assumed that only precipitation isotope measurement at
278 the most downstream site Nuxia is available for the correction of isoGSM (i.e., scenario
279 P_1station in Table 3).

280 *Experiment 3: influence of stream water sampling strategy*

281 The third experiment was conducted to analyze the influence of stream water sampling
282 strategy on the model performance. Two types of stream water sampling strategies were
283 considered, i.e., a time series sampling strategy based on regular and continuous sampling work
284 at a certain point, and a spatially distributed sampling strategy based on one-time field
285 campaigns of sampling work. For the time series sampling strategy, 7 scenarios (scenarios begin
286 with “RT_YTR_” in Table 3) were designed to analyze the influences of the sampling frequency,
287 the duration of the sampling period, and the number of sampling sites. For the spatially



288 distributed sampling strategy, two scenarios (Figure 1b) were designed to represent typical field
289 campaign activities: collecting samples along the mainstream of the basin (RS_YTR_Main,
290 Table 3), and collecting water samples additionally from major tributaries (RS_YTR_Tributary,
291 Table 3). Considering the limited availability of stream water $\delta^{18}\text{O}$ measurement in the YTR
292 basin (only wet season in one year, Table 1), a supplementary experiment was designed to test
293 the influence of sampling period duration on the model performance using the relatively long
294 time-series isotope dataset in the small catchment KR (scenarios begin with “RT_KR_” in Table
295 3).

296 To evaluate the influence of isotope data availability on the model performance, we carried
297 out benchmark model simulations forced by full datasets of input isotope and stream water
298 isotope data in the YTR and KR catchments (Table 3). The benchmark model runs were
299 calibrated by a bi-objective calibration using SCA and streamflow observations, and a tri-
300 objective calibration using additional stream water isotope, respectively. It is noted that, in
301 experiments that were carried out in the YTR basin (i. e., scenarios start with “RT_YTR_” and
302 “RS_YTR_” in Table 3), assumed stream water $\delta^{18}\text{O}$ measurements were adopted from model
303 simulations driven by a benchmark parameter set, which was selected from the behavioral
304 parameters of the BM_YTR calibrated by tri-objective approach, because the assumed data
305 availability was beyond the actual measurement dataset. The assumed stream water $\delta^{18}\text{O}$
306 measurements thus were not used to evaluate the model performance in simulating stream water
307 isotope. Instead, the influence of the availability of stream water $\delta^{18}\text{O}$ measurement on the
308 tracer-aided model were evaluated by comparing the estimated CRCs and corresponding
309 uncertainties with the assumed true values that were derived from the tri-objective calibrated
310 benchmark running. Mean absolute error (MAE) and standard deviation (STD) were used to
311 quantify the accuracy and uncertainty of CRC, which were calculated in Eqs. 9 and 10.

$$312 \quad \text{MAE}^k = \frac{\sum_{i=1}^n |\text{CRC}_{s,i}^k - \text{CRC}_o^k|}{n} \quad (9)$$

$$313 \quad \text{STD}^k = \sqrt{\frac{\sum_{i=1}^n (\text{CRC}_{s,i}^k - \overline{\text{CRC}}_s^k)^2}{n}} \quad (10)$$

314 where, n is the number of behavioral parameter sets, and superscript k indicates the runoff
315 component (one of rainfall, snowmelt, glacier melt and baseflow). Subscript s and o indicate
316 the simulated and observed value (observed value is the CRC produced by the tri-objective
317 calibrated benchmark running). $\text{CRC}_{s,i}^k$ is the contribution of runoff component k simulated by
318 the parameter set i . $\overline{\text{CRC}}_s^k$ is the average CRC simulated by all the behavioral parameter sets.

319 In the remaining experiments in Table 3, the influence of isotope data availability on model
320 performance were quantified by changes in model performance in the validation period and
321 internal validate hydrological stations, as well as the uncertainty of CRC estimated by Eq. 10.

322



323 **3. Results**

324 **3.1 Performance of the tracer-aided hydrological model**

325 Figure 2 shows performance of the benchmark model running (i.e., BM_YTR scenario in
326 Table 3) forced and calibrated by the full available isotope dataset. Seasonal variations in
327 discharge and SCA were reproduced well by the bi-objective calibration (Figure 2a and 2b),
328 indicated by the high values of NSE_{dis} (>0.8) and $\ln NSE_{dis}$ (>0.8), and a low $RMSE_{SCA}$ (<0.08).
329 The peak flows were less well reproduced by the model in comparison to the simulation of
330 baseflow processes, partly due to the inaccurate precipitation input data at the high altitudes.
331 The model showed extremely poor performance for the simulation of stream water isotope
332 when looking at the large uncertainty range (Figure 2c) and low NSE_{iso} (-0.72). The tri-objective
333 calibration significantly improved the isotope simulation (Figure 2f), without bringing much
334 sacrifice to the performance in simulating discharge and SCA (considering the minimum values
335 of NSE_{dis} and $\ln NSE_{dis}$ are around 0.7 in Figure 2d and 2e). Moreover, the tri-objective
336 calibration slightly reduced uncertainty for simulation of the rising hydrograph in the 2009
337 spring (Figure 2d). The seasonal variations in stream water $\delta^{18}O$ were captured well at all the
338 four stations by simulations from the tri-objective calibration. The mean contributions of
339 rainfall and snowmelt to annual streamflow estimated by the bi-objective calibration were 62.8%
340 and 10.8%, which were around 1%-7% smaller than those estimated by the tri-objective
341 calibration (Table 4). In contrast, the contribution of glacier melt estimated by the tri-objective
342 calibration (17.1%) was lower than that estimated by the bi-objective calibration (26.4%).
343 Surface runoff which was mainly fed by glacier melt in the YTR showed a larger proportion in
344 the total streamflow simulated by a bi-objective calibration (52.1%) than that in the simulation
345 of a tri-objective calibration (44.7%), while baseflow contribution quantified by the bi-
346 objective calibration is smaller. Standard deviation values of the quantified CRCs indicated that
347 the tri-objective calibration estimated smaller uncertainties for the quantifications of runoff
348 components. A benchmark parameter set that performed well on multiple objectives was
349 selected among the behavioral parameters of BM_YTR calibrated by tri-objective method (as
350 shown in Table 5), to produce stream water $\delta^{18}O$ for model calibration in experiment 3 in YTR
351 basin.

352 [Figure 2]

353 [Table 4]

354 [Table 5]

355 Figure 3 shows model performances in the KR catchment. Variations of discharge and SCA
356 were reproduced comparably well by the bi- and tri-objective calibrations indicated by the
357 similar metric values. However, the bi-objective calibration produced extremely poor
358 performance for the isotope simulation with low NSE_{iso} and a large simulation error of ~5%



359 (Figure 3c). The tri-objective calibration captured the seasonal variations in stream water $\delta^{18}\text{O}$
360 during the study period well. Similarly to YTR, the tri-objective calibration resulted in lower
361 uncertainty in the simulated hydrograph (e.g., early 2010, 2006 and 2008), benefiting from
362 involving isotope for the model calibration to reject parameter sets that produced good
363 performance for discharge and SCA simulations but poor performance for isotope simulation.
364 Regarding the CRCs to total streamflow, the bi-objective and tri-objective calibrations
365 estimated similar results with differences up to 3%. The mean contributions of rainfall,
366 snowmelt and glacier melt to annual streamflow in the KR catchment were around 45%, 22%
367 and 33%, respectively. Contribution of surface runoff estimated by the bi-objective calibration,
368 however, was 13% lower than that estimated by the tri-objective calibration. In contrast,
369 baseflow is more important in the total streamflow simulated by the bi-objective calibration
370 (accounting for 38%) in comparison to the simulation of the tri-objective calibration
371 (accounting for 25%). Again in the KR catchment, uncertainties of CRCs quantified by the tri-
372 objective calibration are much smaller than those estimated by the bi-objective calibration
373 (Figure 3).

374

[Figure 3]

375 **3.2 Changes in model simulations forced by different assumed glacier meltwater isotopes**

376 Model simulations forced by assumed glacier meltwater $\delta^{18}\text{O}$ that are 5‰ (scenario
377 BM_YTR, $\Delta\delta=5\text{‰}$) and 7‰ (scenario G_Δ7, $\Delta\delta=7\text{‰}$) lower than the long-term average
378 precipitation $\delta^{18}\text{O}$ showed the best discharge simulations in the validation period (2011-2015)
379 and stations (Yangcun and Nugesha), indicated by the high average metric values (Figure 4). It
380 is noted that simulations of all the glacier meltwater isotope input scenarios in experiment 1
381 except G_Δ1 performed better than the bi-objective calibration in which isotope data was not
382 involved for parameter identification. Discharge simulation in the scenario of G_Δ1 estimated
383 higher performance in the validation period than the bi-objective calibration (Figure 4a), but
384 lower performance at internal stations (Figure 4b and 4c).

385

[Figure 4]

386 Figure 5 shows the average CRCs and corresponding uncertainties estimated by the
387 different glacier melt isotope inputs. Scenarios with larger $\Delta\delta$ values (i.e., glacier meltwater
388 isotope is much lower than precipitation isotope) tended to result in higher contributions of
389 precipitation and lower contributions of glacier melt (Figure 5). This can be expected, as stream
390 water $\delta^{18}\text{O}$ is a mixture mainly from $\delta^{18}\text{O}$ of precipitation and glacier meltwater in YTR basin
391 and precipitation $\delta^{18}\text{O}$ is fixed in all the scenarios. Result of scenario G_Δ1, however, estimated
392 a smaller contribution of glacier melt than the scenario G_Δ3. This was likely due to that the
393 behavioral parameter sets were selected based on the performance of both discharge and isotope
394 simulations. Parameter sets that estimated higher glacier melt contribution with good



395 performance in isotope simulation but performed poorly on discharge simulation were excluded
396 from the behavioral set in the G_Δ1 scenario.

397 [Figure 5]

398 3.3 Changes in model performance forced by corrected isoGSM product using different 399 site measurements of precipitation isotope

400 While different scenarios produced similar SCA simulations in the validation period
401 (Figure 6d), the performance of discharge simulation significantly differed among the
402 precipitation isotope input scenarios in experiment 2. In scenarios BM_YTR and P_2stationNL,
403 the model performed better than the bi-objective calibration in the validation period (Figure 6a)
404 and stations (Figure 6b and 6c), showing higher average values and smaller ranges of NSE_{dis} ,
405 which indicated that the model benefitted from involving isotope data for calibration. The
406 model performance forced by scenario P_2stationNY was close to that of the bi-objective
407 calibration. Using precipitation isotope input from the scenario P_1station, however, the model
408 performance was significantly worse than that of the bi-objective calibration. Reasons for the
409 variable model performance forced by the precipitation isotope input scenarios could be: Site
410 measurements of precipitation isotope used in scenarios BM_YTR (using data at four sampling
411 stations) and P_2stationNL (using data at the most downstream sampling station and the most
412 upstream sampling station) tended to provide more informative spatial distribution of
413 precipitation $\delta^{18}O$ in the basin and were the most valuable data for the correction of isoGSM
414 estimate; in the scenario of P_1station, on the contrary, the isoGSM product was inadequately
415 corrected by site precipitation isotope measured only at the most downstream station Nuxia,
416 resulting in much errors in the isoGSM product at high altitudes.

417 [Figure 6]

418 Figure 7 shows the average CRCs and corresponding uncertainties estimated by the
419 different precipitation isotope input scenarios. All scenarios produced lower uncertainties than
420 the bi-objective calibration, which can be expected as they were calibrated by a tri-objective
421 approach. The variable precipitation input scenarios resulted in contribution differences of
422 around 10% in runoff components of rainfall, glacier melt and baseflow. Different site
423 measurements of precipitation isotope that were used for the correction of isoGSM product
424 resulted in different altitudinal lapse rates in the corrected isoGSM input (i.e., parameter a in
425 equation 2); and scenario P_1station estimated the most overestimated average precipitation
426 $\delta^{18}O$ ($\overline{\delta^{18}O_{precipitation}}$), while scenario P_2stationNL estimated the lowest $\overline{\delta^{18}O_{precipitation}}$,
427 leading to varied precipitation contributions to streamflow.

428 [Figure 7]

429 Among the evaluation metrics, discharge simulation at Nugesha station showed the largest



430 sensitivity to precipitation isotope inputs. As shown in Figure 8, scenarios P_2stationNY and
431 P_1station estimated higher contribution of meltwater, earlier discharge onset timing and higher
432 peak flow. The discharge began to rise especially early (around February) in scenario P_1station,
433 because of the low calibrated value for the melting temperature threshold T_0 (-4.5°C), resulted
434 in extremely poor discharge simulation (average NSE is around 0, Figure 8d).

435 **[Figure 8]**

436 **3.4 Model performance constrained by different stream water sampling strategies**

437 Figure 9 shows the accuracy and uncertainty metrics of CRCs produced by experiment 3
438 in the YTR basin. In comparison to the baseline scenario of RT_TYR_BM, collecting stream
439 isotope data in the dry season (i.e., from November to next February in scenario
440 RT_YTR_WholeYear) brought little benefits to the estimation of water sources proportions, but
441 significantly improved the quantifications of runoff generation pathways indicated by the lower
442 MAE and STD in Figure 9b. The stream water in dry season was fed mainly by groundwater.
443 Stream water isotope data collected in this period reflect the release of groundwater storage,
444 thus helping to constrain the partition between surface and subsurface runoff pathway. On the
445 other hand, reducing the frequency of stream isotope data from weekly to monthly (i.e., scenario
446 RT_YTR_Monthly) led to significantly higher MAE and STD for both the partitions of water
447 sources and runoff pathways, which indicated that stream water isotope data collected by a
448 monthly sampling strategy could provide less constrains to model calibration. Extending the
449 duration of stream isotope sampling period by one or two years (i.e., scenarios RT_YTR_2year
450 and RT_YTR_3year) did not bring much benefits to the quantifications of CRCs regarding the
451 similar metric values. Using stream water isotope data from a three years' sampling
452 (RT_YTR_3year) even led to higher MAE and STD than that using stream water isotope data
453 from a 2 years' sampling (RT_YTR_2year), which might be an occasional result obtained by
454 the random calibration procedure (100 pySOT runs). In comparison to simulations constrained
455 by stream water isotope data from multiple sampling years, results constrained by stream water
456 isotope data from multiple sampling sits (i.e., scenarios of RT_YTR_2station and
457 RT_YTR_4station) yielded lower MAE and STD for the quantified CRCs.

458 **[Figure 9]**

459 Model simulations calibrated by spatially distributed stream $\delta^{18}\text{O}$ data collected in a one-
460 time field campaign reduced the CRC uncertainty compared to the bi-objective calibration
461 (Figure 9). However, its MAE and STD for the quantifications of CRCs were higher than that
462 estimated by the model when calibrated by weekly sampled time series of stream $\delta^{18}\text{O}$.
463 Additionally using stream isotope data from four major tributaries (i.e., scenario
464 RS_YTR_Tributary) brought little benefits to the model performance than using isotope data
465 from the main stream solely (RS_YTR_Main), partly due to the signatures of stream water



466 isotope from tributaries were already reflected by water samples collected at confluences on
467 the main river channel.

468 In the KR catchment, stream isotope data was collected from five continuous years,
469 providing better data basis for the evaluation of the influence of sampling period duration.
470 Figure 10 and 11 compare the CRC estimations and their uncertainty metric STD of variable
471 scenarios. For the estimate of water sources, the model produced rather large uncertainty ranges
472 of ~20% and ~40% for the contributions of rainfall and glacier melt when calibrating the model
473 using discharge and SCA. Using one-year's stream water isotope data for model calibration,
474 the uncertainty ranges were reduced by rejecting some outliers as shown in Figure 10a-c, but
475 the STD was still large (Figure 11). The STD can be reduced by increasing the number of
476 calibration isotope data at a rate of ~1%/year. Using isotope data collected from five years,
477 however, didn't result in further decrease in the CRC uncertainties compared to the result
478 calibrated by isotope data collected in a four-year sampling period. The situation, however, was
479 quite different for the estimates of runoff pathways. The bi-objective calibration produced a
480 large uncertainty of ~40% and a STD of ~10% (Figure 10d) for the contribution of baseflow.
481 Using one-year's data for model calibration, the uncertainty range was significantly reduced by
482 about half of that modelled by the bi-objective calibration (from ~10% to ~5%). However,
483 further increase in the duration of sampling period did not bring much improvements on
484 constraining the uncertainties in quantifications of runoff pathways with STD fluctuating
485 around only 4%. It is indicated that model calibration upon more stream isotope data was useful
486 to better constrain the uncertainties of the model simulations and modeled CRCs, but benefit
487 would disappear after a certain duration of stream water sampling period has been reached.

488 [Figure 10]

489 [Figure 11]

490 **4. Discussions**

491 **4.1 Implications for water sampling for isotope analysis in high mountains of TP**

492 This study tested the reliance of the benefits of using tracer-aided hydrological model on
493 isotope data availability in two mountainous catchments YTR and KR on the TP. Our findings
494 consistently showed that the model robustness, with respect to performance in the validation
495 period and internal stations and the quantifications of CRCs, can be significantly improved by
496 involving isotope data for parameter calibration, similarly to previous tracer-aided modeling
497 studies (e.g., He et al., 2019; Ala-aho et al., 2017; Birkel et al., 2010). It can be expected that
498 more data help to provide more constraints on identification of model parameters. Nonetheless,
499 water sampling in high mountains on the TP is restricted by environment accessibility, financial
500 and human costs (Stevenson et al., 2021, Li et al., 2020). It is therefore highly needed to find



501 optimal strategies of collecting water samples that balance well between data adequacy for
502 model running and affordable sampling cost (Sprenger et al., 2019).

503 As an important water source in mountainous catchment on the TP, sampling of glacier
504 meltwater was expected to be favorable for the determination of glacier meltwater isotopic
505 composition and its contribution to total streamflow (He et al., 2019). Field campaign for
506 sampling of glacier melt water is strongly challenging in the YTR basin in this study, due to the
507 harsh accessibility of very high altitudes where glaciers lie. We thus assumed that glacier
508 meltwater $\delta^{18}\text{O}$ was lower than the average local precipitation $\delta^{18}\text{O}$ by an offset parameter ($\Delta\delta$).
509 This simple assumption turned to work well on driving the tracer-aided hydrological model and
510 produced better performance than the bi-objective calibration in both validation periods and
511 internal stations. Experiments by using different $\Delta\delta$ values indicated that the prior assumed
512 isotopic compositions of glacier melt have small influence on the estimated glacier meltwater
513 contribution in the YTR basin. The $\Delta\delta$ values ranging from 2‰-9‰ led to only ~5% difference
514 in the estimated contributions of glacier melt. Using a $\Delta\delta$ to estimate glacier meltwater $\delta^{18}\text{O}$
515 could serve as an option to force the tracer-aided hydrological models in high-mountain
516 catchments where collecting glacier meltwater samples is highly challenging.

517 Results of experiment 2 indicated that the original isoGSM precipitation $\delta^{18}\text{O}$ data showed
518 large bias in the high mountain basins on TP, and must undergo correction before using to force
519 the tracer-aided hydrological model. Our experiments showed that measurement of
520 precipitation isotope at only two sampling sites (scenario P_2stationNL) in the large YTR basin
521 of $2 \times 10^5 \text{ km}^2$ can be highly valuable for the correction of isoGSM product. Forced by isoGSM
522 data that was corrected by precipitation $\delta^{18}\text{O}$ measurements from two sampling sites, the model
523 performed better than the bi-objective calibration in simulating discharge in the validation
524 period and internal stations, and performed comparably to the simulations of a benchmark
525 running which used precipitation $\delta^{18}\text{O}$ measurements from four stations for the isoGSM
526 correction. This benefitted from the large altitudinal range covered by the two sampling sites (a
527 most downstream site Nuxia and a most upstream site Lazi) to represent the spatial pattern of
528 isoGSM bias. Likewise using measurement data at two sites in the scenario P_2stationNY,
529 model performance deteriorated visibly, as the sampling sites (Nuxia and Yangchun) were both
530 located in the downstream regions, being worse at representing the spatial pattern of
531 precipitation $\delta^{18}\text{O}$ over the basin. Consequently, the strategy of collecting precipitation samples
532 to correct isoGSM should be carefully designed; spending high cost on collecting precipitation
533 samples within a small region might be not worth at improving the performance of the tracer-
534 aided hydrological model.

535 Measurements of stream water $\delta^{18}\text{O}$ are essential for the calibration and evaluation of
536 tracer-aided hydrological models. Three kinds of sampling strategies in YTR basin were
537 evaluated in experiment 3: one-time campaign field sampling, continuous sampling at a fixed



538 location for a long period, and continuous sampling at multiple fixed locations during a short
539 period. It is indicated that continuously sampled stream water $\delta^{18}\text{O}$ at a fix location is more
540 valuable for aiding hydrological model than that collected by one-time field sampling
541 campaigns at distributed sites. Seasonality of stream water $\delta^{18}\text{O}$ referring to the processes of
542 water storage, mixture and transport in the basin can be better captured by continuous time
543 series measurements of $\delta^{18}\text{O}$ data (McGuire and McDonnell, 2006). Spatially sampled stream
544 water $\delta^{18}\text{O}$ data by one-time field sampling campaigns possibly miss seasonal $\delta^{18}\text{O}$ signatures
545 of stream water that were caused by seasonal runoff generation processes (Kendall and Coplen,
546 2001; Nan et al., 2019), and provide less constrains for the model calibration. Sampling of
547 stream water during dry season (scenario RT_YTR_WholeYear) brought little improvements
548 to the modeling of water source proportions, which is consistent with the findings in Stevenson
549 et al. (2021). High frequent like weekly sampling of stream water in the dry season makes small
550 senses on improving the stream $\delta^{18}\text{O}$ data quality, as stream $\delta^{18}\text{O}$ in this season has little
551 variations due to small precipitation triggered runoff inputs. Monthly sampling of stream water
552 (RT_YTR_Monthly) turned to be insufficient to capture the strong hydrological variations in
553 the wet season (Birkel and Soulsby, 2015). For large basins like YTR, increasing the number
554 of sampling site for stream water $\delta^{18}\text{O}$ is more useful than extending the years of sampling
555 period at fixed sites, as seasonality of $\delta^{18}\text{O}$ signatures of water sources should be similar among
556 years in a short study period. Consequently, continuous sampling at multiple locations in a short
557 period like one or two years seems to be the optimal stream sampling strategy for running
558 tracer-aided hydrological model in mountainous basins like YTR on the TP. The value of
559 extending sampling period was more significant in a smaller catchment KR. The uncertainty of
560 CRC estimation kept decreasing until the data series length reached four years and two years,
561 for the aspects of water source and runoff pathway, respectively. This was consistent with the
562 finding by Stevenson et al. (2021) that the benefits from isotope plateaued after a certain year
563 number, which was five for that study.

564 4.2 Uncertainties and limitations

565 This study used simulated stream $\delta^{18}\text{O}$ of a benchmark model running to represent the fully
566 available dataset of stream $\delta^{18}\text{O}$ for water sampling in the YTR basin, due to the limited stream
567 water samples. This procedure likely caused the inherent correlation of the stream $\delta^{18}\text{O}$ dataset,
568 which made the model easily reproduce the assumed measurements of stream $\delta^{18}\text{O}$ and may
569 underestimate the value of stream $\delta^{18}\text{O}$ data collected in extended sampling years and sampling
570 sites. Results in this study serve to provide preliminary understandings of the influences of
571 stream water sampling strategy on the model performance. More solid evaluations, however,
572 can be further benefited from using more real field measurements of stream $\delta^{18}\text{O}$ in the
573 mountain basins.



574 Our study tried to look for optimal water sampling strategies to provide isotope input and
575 calibration data for the tracer-aided hydrological model in the YTR basin and KR catchment on
576 the TP. The transferability of our findings to other basins can be partly expected. For example,
577 we can expect that in catchments where precipitation $\delta^{18}\text{O}$ and runoff processes show small
578 spatial heterogeneity, collecting water samples at multiple stations would bring few additional
579 benefits for the modeling work than collecting water samples at a sole station. The influence of
580 assumed glacier meltwater would differ with the glacier covered area fraction in the basins.
581 However, situations in catchments with different geographical and climatic characteristics were
582 not evaluated in this study, which is restricted by the fact that high-quality water isotope data
583 in a set of mountain basins on the TP were hardly available currently (Birkel and Soulsby, 2015).
584 The authors suggest tracer-aided modeling researchers to publish their water isotope data to
585 improve the evaluation of the reliance of tracer-aided modeling performance on water sampling
586 strategy (similarly to He et al. 2021; Niinikoski et al., 2016; Yde et al., 2016).

587 5. Conclusion

588 The value of water isotope data for aiding hydrological modeling in large mountainous
589 catchments was tested by a set of numerical experiments in the YTR basin. Reliance of the
590 tracer-aided model performance on the availability of input isotope data and evaluation stream
591 water isotope data was extensively investigated in the numerical experiments. Results could
592 provide important guidance for water sampling in mountainous regions on the TP. Our main
593 finds are as follows:

594 1. In high-mountain basins where glacier meltwater samples for isotope analysis are not
595 available, estimating isotopic composition of glacier meltwater by an offset parameter from
596 precipitation isotope is a feasible way to force the tracer-aided hydrological model. Our test
597 indicated that using a set of glacier meltwater $\delta^{18}\text{O}$ that are 2‰~9‰ lower than the mean
598 precipitation $\delta^{18}\text{O}$, resulted in small changes in the model performance and the quantifications
599 of CRCs (smaller than 5%) in the YTR basin. This influence, however, is expected to change
600 with the glacier area coverages in other mountain basins.

601 2. Strategy of field sampling for precipitation to correct the isoGSM product should be
602 carefully designed. Collecting precipitation samples at sites from the same altitude tends to be
603 worse at representing the spatial pattern of precipitation $\delta^{18}\text{O}$ over the basin than collecting
604 precipitation samples from sites covering a range of altitudes. Measurements of precipitation
605 isotope at only two sampling sites covering an elevation range of 2900-6900m in the large YTR
606 basin of $2 \times 10^5 \text{ km}^2$ can be highly valuable for the correction of isoGSM product.

607 3. Collecting weekly stream water samples at multiple sites in the wet and warm seasons is
608 the optimal strategy for calibrating and evaluating a tracer-aided hydrological model in the YTR
609 basin. It is highly recommended to increase the number of stream water sampling sites in the



610 high-mountain basins rather than extending the duration of sampling period at a sole site.
611 Benefits from extending the duration of sampling period is more visible in a small catchment
612 but smaller in large basins, and tend to disappear when a certain duration of sampling period
613 has been reached.

614

615 **Code and data availability**

616 Code and data availability. The isotope data and the code of THREW-T model used in this study
617 are available from the corresponding author (tianfq@tsinghua.edu.cn). Other data sets and the
618 calibration program pySOT are publicly available as follows: DEM
619 (<http://www.gslcloud.cn/sources/details/310?pid=302>, last access: 1 January 2019, Geospatial
620 Data Cloud Site, 2019), CMFD (<https://doi.org/10.11888/AtmosphericPhysics.tpe.249369.file>,
621 Yang and He, 2019), glacier data (<https://doi.org/10.3972/glacier.001.2013.db>, Liu et al., 2012),
622 NDVI (<https://doi.org/10.5067/MODIS/MOD13A3.006>, Didan et al., 2015), LAI
623 (<https://doi.org/10.5067/MODIS/MOD15A2H.006>, Myneni et al., 2015), HWSD
624 (<https://data.tpdac.ac.cn/zh-hans/data/3519536a-d1e7-4ba1-8481-6a0b56637baf/?q=HWSD>,
625 last access: 1 January 2019, He, 2019) and the pySOT program
626 (<https://doi.org/10.5281/zenodo.569554>, Eriksson et al., 2017). These data sets and programs
627 are also referred to in the main text (Yang et al., 2010; Chen et al., 2018).

628 **Author contribution**

629 YN, ZH and FT conceived the idea; ZW provided the isoGSM data; LT provided the
630 measurement isotope data; YN, ZH and FT conducted analysis; ZW and LT provided comments
631 on the analysis; all the authors contributed to writing and revisions.

632 **Financial support**

633 This study has been supported by the National Natural Science Foundation of China (grant no.
634 92047301).

635 **Competing interests**

636 At least one of the (co-)authors is a member of the editorial board of Hydrology and Earth
637 System Sciences.

638

639 **References**

640 Ala-aho, P., Tetzlaff, D., McNamara, J. P., Laudon, H., and Soulsby, C.: Using isotopes to
641 constrain water flux and age estimates in snow-influenced catchments using the STARR
642 (Spatially distributed Tracer-Aided Rainfall–Runoff) model, *Hydrology and Earth System
643 Sciences*, 21, 5089–5110, 10.5194/hess-21-5089-2017, 2017.



- 644 Birkel, C., Dunn, S. M., Tetzlaff, D., and Soulsby, C.: Assessing the value of high-resolution
645 isotope tracer data in the stepwise development of a lumped conceptual rainfall-runoff
646 model, *Hydrological Processes*, 24, 2335-2348, 10.1002/hyp.7763, 2010.
- 647 Birkel, C., Tetzlaff, D., Dunn, S. M., and Soulsby, C.: Using time domain and geographic source
648 tracers to conceptualize streamflow generation processes in lumped rainfall-runoff models,
649 *Water Resources Research*, 47, 10.1029/2010wr009547, 2011.
- 650 Birkel, C., and Soulsby, C.: Advancing tracer-aided rainfall-runoff modelling: a review of
651 progress, problems and unrealised potential, *Hydrological Processes*, 29, 5227-5240,
652 10.1002/hyp.10594, 2015.
- 653 Bloeschl, G., and Montanari, A.: Climate change impact: throwing the dice?, *Hydrological*
654 *Processes*, n/a-n/a, 10.1002/hyp.7574, 2009.
- 655 Boral, S., and Sen, I. S.: Tracing 'Third Pole' ice meltwater contribution to the Himalayan rivers
656 using oxygen and hydrogen isotopes, *Geochemical Perspectives Letters*, 48-53,
657 10.7185/geochemlet.2013, 2020.
- 658 Bowen, G. J., Cai, Z., Fiorella, R. P., and Putman, A. L.: Isotopes in the Water Cycle: Regional-
659 to Global-Scale Patterns and Applications, in: *Annual Review Of Earth And Planetary*
660 *Sciences*, Vol 47, edited by: Jeanloz, R., and Freeman, K. H., *Annual Review of Earth and*
661 *Planetary Sciences*, 453-+, 2019.
- 662 Capell, R., Tetzlaff, D., and Soulsby, C.: Can time domain and source area tracers reduce
663 uncertainty in rainfall - runoff models in larger heterogeneous catchments?, *Water*
664 *Resources Research*, 48, 10.1029/2011wr011543, 2012.
- 665 Chen, X., Long, D., Hong, Y., Zeng, C., and Yan, D.: Improved modeling of snow and glacier
666 melting by a progressive two-stage calibration strategy with GRACE and multisource data:
667 How snow and glacier meltwater contributes to the runoff of the Upper Brahmaputra River
668 basin?, *Water Resources Research*, 53, 2431-2466, 10.1002/2016wr019656, 2017.
- 669 Chen, X., Long, D., Liang, S., He, L., Zeng, C., Hao, X., and Hong, Y.: Developing a composite
670 daily snow cover extent record over the Tibetan Plateau from 1981 to 2016 using
671 multisource data, *Remote Sen. Environ.*, 215, 284-299,
672 <https://doi.org/10.1016/j.rse.2018.06.021>, 2018.
- 673 Delavau, C. J., Stadnyk, T., and Holmes, T.: Examining the impacts of precipitation isotope
674 input on distributed, tracer-aided hydrological modelling, *Hydrology and Earth System*
675 *Sciences*, 21, 2595-2614, 10.5194/hess-21-2595-2017, 2017.
- 676 Didan, K.: MOD13A3 MODIS/Terra vegetation Indices Monthly L3 Global 1km SIN Grid
677 V006, NASA EOSDIS Land Processes DAAC [data set],
678 <https://doi.org/10.5067/MODIS/MOD13A3.006>, 2015.
- 679 Dong, G., Weng, B., Chen, J., Yan, D., and Wang, H.: Variation characteristics of stable isotopes
680 in water along main stream of Naqu River in source area of Nujiang River, *Water*



- 681 Resources and Hydropower Engineering, 49, 108-114, 2018.
- 682 Duethmann, D., Bolch, T., Farinotti, D., Kriegel, D., Vorogushyn, S., Merz, B., Pieczonka, T.,
683 Jiang, T., Su, B., and Guentner, A.: Attribution of streamflow trends in snow and glacier
684 melt-dominated catchments of the Tarim River, Central Asia, Water Resources Research,
685 51, 4727-4750, 10.1002/2014wr016716, 2015.
- 686 Dunn, S. M., McDonnell, J. J., and Vaché, K. B.: Factors influencing the residence time of
687 catchment waters: A virtual experiment approach, Water Resources Research, 43,
688 10.1029/2006wr005393, 2007.
- 689 Eriksson, D., Bindel, D., and Shoemaker, C.: Dme65/Pysot: V0.1.35, Zenodo [code],
690 <https://doi.org/10.5281/zenodo.569554>, 2017.
- 691 Gao J., Tian L., and Liu, Y.: Oxygen isotope variation in the water cycle of the Yamzho Lake
692 Basin in southern Tibetan Plateau, Chinese Sci. Bull., 54, 2758–2765, 2009.
- 693 Gupta, H. V., Wagener, T., and Liu, Y.: Reconciling theory with observations: elements of a
694 diagnostic approach to model evaluation, Hydrological Processes, 22, 3802-3813,
695 10.1002/hyp.6989, 2008.
- 696 He, Y.: Pan-TPE soil map based on Harmonized World Soil Database (V1.2), National Tibetan
697 Plateau Data Center [data set], [https://data.tpcd.ac.cn/zh-hans/data/3519536a-d1e7-4ba1-](https://data.tpcd.ac.cn/zh-hans/data/3519536a-d1e7-4ba1-8481-6a0b56637baf/?q=HWSD)
698 [8481-6a0b56637baf/?q=HWSD](https://data.tpcd.ac.cn/zh-hans/data/3519536a-d1e7-4ba1-8481-6a0b56637baf/?q=HWSD), 2019
- 699 He, Z. H., Tian, F. Q., Gupta, H. V., Hu, H. C., and Hu, H. P.: Diagnostic calibration of a
700 hydrological model in a mountain area by hydrograph partitioning, Hydrology and Earth
701 System Sciences, 19, 1807-1826, 10.5194/hess-19-1807-2015, 2015.
- 702 He, Z., Unger-Shayesteh, K., Vorogushyn, S., Weise, S. M., Kalashnikova, O., Gafurov, A.,
703 Duethmann, D., Barandun, M., and Merz, B.: Constraining hydrological model parameters
704 using water isotopic compositions in a glacierized basin, Central Asia, Journal of
705 Hydrology, 571, 332-348, 10.1016/j.jhydrol.2019.01.048, 2019.
- 706 He, Z., Unger-Shayesteh, K., Vorogushyn, S., Weise, S. M., Duethmann, D., Kalashnikova, O.,
707 Gafurov, A., and Merz, B.: Comparing Bayesian and traditional end-member mixing
708 approaches for hydrograph separation in a glacierized basin, Hydrology and Earth System
709 Sciences, 24, 3289-3309, 10.5194/hess-24-3289-2020, 2020.
- 710 He, Z., Duethmann, D., and Tian, F.: A meta-analysis based review of quantifying the
711 contributions of runoff components to streamflow in glacierized basins, Journal of
712 Hydrology, 603, 126890, 10.1016/j.jhydrol.2021.126890, 2021.
- 713 Hindshaw, R. S., Tipper, E. T., Reynolds, B. C., Lemarchand, E., Wiederhold, J. G., Magnusson,
714 J., Bernasconi, S. M., Kretzschmar, R., and Bourdon, B.: Hydrological control of stream
715 water chemistry in a glacial catchment (Damma Glacier, Switzerland), Chemical Geology,
716 285, 215-230, 10.1016/j.chemgeo.2011.04.012, 2011.
- 717 Immerzeel, W. W., van Beek, L. P. H., and Bierkens, M. F. P.: Climate Change Will Affect the



- 718 Asian Water Towers, *Science*, 328, 1382-1385, 10.1126/science.1183188, 2010.
- 719 Jeelani, G., Shah, R. A., Jacob, N., and Deshpande, R. D.: Estimation of snow and glacier melt
720 contribution to Liddar stream in a mountainous catchment, western Himalaya: an isotopic
721 approach, *Isotopes in environmental and health studies*, 53, 18-35,
722 10.1080/10256016.2016.1186671, 2017.
- 723 Kendall, C., and Coplen, T. B.: Distribution of oxygen-18 and deuterium in river waters across
724 the United States, *Hydrological Processes*, 15, 1363-1393, 10.1002/hyp.217, 2001.
- 725 Klaus, J., and McDonnell, J. J.: Hydrograph separation using stable isotopes: Review and
726 evaluation, *Journal of Hydrology*, 505, 47-64, 10.1016/j.jhydrol.2013.09.006, 2013.
- 727 Knapp, J. L. A., Neal, C., Schlumpf, A., Neal, M., and Kirchner, J. W.: New water fractions and
728 transit time distributions at Plynlimon, Wales, estimated from stable water isotopes in
729 precipitation and streamflow, *Hydrology and Earth System Sciences*, 23, 4367-4388,
730 10.5194/hess-23-4367-2019, 2019.
- 731 Kong, Y., Wang, K., Pu, T., and Shi, X.: Nonmonsoon Precipitation Dominates Groundwater
732 Recharge Beneath a Monsoon-Affected Glacier in Tibetan Plateau, *Journal of Geophysical
733 Research: Atmospheres*, 124, 10913-10930, 10.1029/2019jd030492, 2019.
- 734 Laudon, H., Taberman, I., Ågren, A., Futter, M., Ottosson-Löfvenius, M., and Bishop, K.: The
735 Krycklan Catchment Study-A flagship infrastructure for hydrology, biogeochemistry, and
736 climate research in the boreal landscape, *Water Resources Research*, 49, 7154-7158,
737 10.1002/wrcr.20520, 2013.
- 738 Li, Z.-J., Li, Z.-X., Song, L.-L., Gui, J., Xue, J., Zhang, B. J., and Gao, W. D.: Hydrological
739 and runoff formation processes based on isotope tracing during ablation period in the
740 source regions of Yangtze River, *Hydrology and Earth System Sciences*, 24, 4169-4187,
741 10.5194/hess-24-4169-2020, 2020.
- 742 Li, Z., Feng, Q., Li, Z., Yuan, R., Gui, J., and Lv, Y.: Climate background, fact and hydrological
743 effect of multiphase water transformation in cold regions of the western china: a review,
744 *EARTH ENCOUNTERS REVIEWS*, 190, 33-57, <https://doi.org/10.1016/j.earscirev.2018.12.004>,
745 2019.
- 746 Liu, S.: The second glacier inventory dataset of China (version 1.0) (2006–2011), National
747 Tibetan Plateau Data Center [data set], <https://doi.org/10.3972/glacier.001.2013.db>, 2012.
- 748 Liu, Z., Tian, L., Yao, T., Gong, T., Yin, C., and Yu, W.: Temporal and spatial variations of delta
749 O-18 in precipitation of the Yarlung Zangbo River Basin, *J. Geogr. Sci.*, 17, 317–326,
750 <https://doi.org/10.1007/s11442-007-0317-1>, 2007.
- 751 Lutz, A. F., Immerzeel, W. W., Shrestha, A. B., and Bierkens, M. F. P.: Consistent increase in
752 High Asia's runoff due to increasing glacier melt and precipitation, *Nature Climate Change*,
753 4, 587-592, 10.1038/nclimate2237, 2014.
- 754 McGuire, K. J., and McDonnell, J. J.: A review and evaluation of catchment transit time



- 755 modeling, *Journal of Hydrology*, 330, 543-563, 10.1016/j.jhydrol.2006.04.020, 2006.
- 756 McGuire, K. J., Weiler, M., and McDonnell, J. J.: Integrating tracer experiments with modeling
757 to assess runoff processes and water transit times, *Advances in Water Resources*, 30, 824-
758 837, 10.1016/j.advwatres.2006.07.004, 2007.
- 759 Myneni, R., Knyazikhin, Y., and Park, T.: MOD15A2H MODIS/Terra Leaf Area Index/FPAR
760 8-Day L4 Global 500m SIN Grid V006, NASA EOSDIS Land Processes DAAC [data set],
761 <https://doi.org/10.5067/MODIS/MOD15A2H.006>, 2015.
- 762 Nan, Y., Tian, F., Hu, H., Wang, L., and Zhao, S.: Stable Isotope Composition of River Waters
763 across the World, *Water*, 11, 1760, 10.3390/w11091760, 2019.
- 764 Nan, Y., He, Z., Tian, F., Wei, Z., and Tian, L.: Can we use precipitation isotope outputs of
765 isotopic general circulation models to improve hydrological modeling in large
766 mountainous catchments on the Tibetan Plateau?, *Hydrology and Earth System Sciences*,
767 25, 6151-6172, 10.5194/hess-25-6151-2021, 2021b.
- 768 Nan, Y., Tian, L., He, Z., Tian, F., and Shao, L.: The value of water isotope data on improving
769 process understanding in a glacierized catchment on the Tibetan Plateau, *Hydrology and
770 Earth System Sciences*, 25, 3653-3673, 10.5194/hess-25-3653-2021, 2021a.
- 771 Niinikoski, P. I. A., Hendriksson, N. M., and Karhu, J. A.: Using stable isotopes to resolve
772 transit times and travel routes of river water: a case study from southern Finland, *Isotopes
773 in environmental and health studies*, 52, 380-392, 10.1080/10256016.2015.1107553, 2016.
- 774 Ohlanders, N., Rodriguez, M., and McPhee, J.: Stable water isotope variation in a Central
775 Andean watershed dominated by glacier and snowmelt, *Hydrology and Earth System
776 Sciences*, 17, 1035-1050, 10.5194/hess-17-1035-2013, 2013.
- 777 Pomeroy, J. W., Gray, D. M., Brown, T., Hedstrom, N. R., Quinton, W. L., Granger, R. J., and
778 Carey, S. K.: The cold regions hydrological model: a platform for basing process
779 representation and model structure on physical evidence, *Hydrological Processes*, 21,
780 2650-2667, 10.1002/hyp.6787, 2007.
- 781 Rai, S. P., Singh, D., Jacob, N., Rawat, Y. S., Arora, M., and BhishmKumar: Identifying
782 contribution of snowmelt and glacier melt to the Bhagirathi River (Upper Ganga) near
783 snout of the Gangotri Glacier using environmental isotopes, *Catena*, 173, 339-351,
784 10.1016/j.catena.2018.10.031, 2019.
- 785 Reggiani, P., Hassanizadeh, S. M., Sivapalan, M., and Gray, W. G.: A unifying framework for
786 watershed thermodynamics: constitutive relationships, *Advances In Water Resources*, 23,
787 15-39, 10.1016/s0309-1708(99)00005-6, 1999.
- 788 Son, K., and Sivapalan, M.: Improving model structure and reducing parameter uncertainty in
789 conceptual water balance models through the use of auxiliary data, *Water Resources
790 Research*, 43, 10.1029/2006wr005032, 2007.
- 791 Sprenger, M., Stumpp, C., Weiler, M., Aeschbach, W., Allen, S. T., Benettin, P., Dubbert, M.,



- 792 Hartmann, A., Hrachowitz, M., Kirchner, J. W., McDonnell, J. J., Orłowski, N., Penna, D.,
793 Pfahl, S., Rinderer, M., Rodriguez, N., Schmidt, M., and Werner, C.: The Demographics
794 of Water: A Review of Water Ages in the Critical Zone, *Reviews Of Geophysics*, 57, 800-
795 834, 10.1029/2018rg000633, 2019.
- 796 Stevenson, J. L., Birkel, C., Neill, A. J., Tetzlaff, D., and Soulsby, C.: Effects of streamflow
797 isotope sampling strategies on the calibration of a tracer-aided rainfall-runoff model,
798 *Hydrological Processes*, 35, 10.1002/hyp.14223, 2021.
- 799 Tan, H., Chen, X., Shi, D., Rao, W., Liu, J., Liu, J., Eastoe, C. J., and Wang, J.: Base flow in the
800 Yarlungzangbo River, Tibet, maintained by the isotopically-depleted precipitation and
801 groundwater discharge, *The Science of the total environment*, 759, 143510,
802 10.1016/j.scitotenv.2020.143510, 2021.
- 803 Tetzlaff, D., Birkel, C., Dick, J., Geris, J., and Soulsby, C.: Storage dynamics in
804 hypopedological units control hillslope connectivity, runoff generation, and the evolution
805 of catchment transit time distributions, *Water Resour Res*, 50, 969-985,
806 10.1002/2013WR014147, 2014.
- 807 Tian, F., Hu, H., Lei, Z., and Sivapalan, M.: Extension of the Representative Elementary
808 Watershed approach for cold regions via explicit treatment of energy related processes,
809 *Hydrology And Earth System Sciences*, 10, 619-644, 10.5194/hess-10-619-2006, 2006.
- 810 Tian, F., Xu, R., Nan, Y., Li, K., and He, Z.: Quantification of runoff components in the Yarlung
811 Tsangpo River using a distributed hydrological model, *Advances in Water Science*, 31,
812 324-336, 2020.
- 813 Tong, R., Parajka, J., Salentinig, A., Pfeil, I., Komma, J., Széles, B., Kubáň, M., Valent, P.,
814 Vreugdenhil, M., Wagner, W., and Blöschl, G.: The value of ASCAT soil moisture and
815 MODIS snow cover data for calibrating a conceptual hydrologic model, *Hydrology and
816 Earth System Sciences*, 25, 1389-1410, 10.5194/hess-25-1389-2021, 2021.
- 817 Viviroli, D., Weingartner, R., and Messerli, B.: Assessing the hydrological significance of the
818 world's mountains, *Mountain Research And Development*, 23, 32-40, 10.1659/0276-
819 4741(2003)023[0032:athsot]2.0.co;2, 2003.
- 820 Wang, C., Dong, Z., Qin, X., Zhang, J., Du, W., and Wu, J.: Glacier meltwater runoff process
821 analysis using δD and $\delta 18O$ isotope and chemistry at the remote Laohugou glacier basin
822 in western Qilian Mountains, China, *Journal of Geographical Sciences*, 26, 722-734,
823 10.1007/s11442-016-1295-y, 2016.
- 824 Wang, Y., Wang, L., Zhou, J., Yao, T., Yang, W., Zhong, X., Liu, R., Hu, Z., Luo, L., Ye, Q.,
825 Chen, N., and Ding, H.: Vanishing Glaciers at Southeast Tibetan Plateau Have Not Offset
826 the Declining Runoff at Yarlung Zangbo, *Geophysical Research Letters*, 48,
827 10.1029/2021gl094651, 2021.
- 828 Wolfe, B. B., Karst-Riddoch, T. L., Hall, R. I., Edwards, T. W. D., English, M. C., Palmimi, R.,



- 829 McGowan, S., Leavitt, P. R., and Vardy, S. R.: Classification of hydrological regimes of
830 northern floodplain basins (Peace–Athabasca Delta, Canada) from analysis of stable
831 isotopes ($\delta^{18}\text{O}$, $\delta^2\text{H}$) and water chemistry, *Hydrological Processes*, 21, 151–168,
832 10.1002/hyp.6229, 2007.
- 833 Xi, X.: A Review of Water Isotopes in Atmospheric General Circulation Models: Recent
834 Advances and Future Prospects, *International Journal of Atmospheric Sciences*, 2014, 1–
835 16, 10.1155/2014/250920, 2014.
- 836 Xia, X., Li, S., Wang, F., Zhang, S., Fang, Y., Li, J., Michalski, G., and Zhang, L.: Triple oxygen
837 isotopic evidence for atmospheric nitrate and its application in source identification for
838 river systems in the Qinghai-Tibetan Plateau, *The Science of the total environment*, 688,
839 270–280, 10.1016/j.scitotenv.2019.06.204, 2019.
- 840 Xu, R., Hu, H., Tian, F., Li, C., and Khan, M. Y. A.: Projected climate change impacts on future
841 streamflow of the Yarlung Tsangpo-Brahmaputra River, *Global and Planetary Change*, 175,
842 144–159, 10.1016/j.gloplacha.2019.01.012, 2019.
- 843 Yang, K. and He, J.: China meteorological forcing dataset (1979–2018), National Tibetan
844 Plateau Data Center [data set],
845 <https://doi.org/10.11888/AtmosphericPhysics.tpe.249369.file>, 2019.
- 846 Yao, T., Masson-Delmotte, V., Gao, J., Yu, W., Yang, X., Risi, C., Sturm, C., Werner, M., Zhao,
847 H., He, Y., Ren, W., Tian, L., Shi, C., and Hou, S.: A review of climatic controls on $\delta^{18}\text{O}$
848 in precipitation over the Tibetan Plateau: Observations and simulations, *Reviews of*
849 *Geophysics*, 51, 525–548, 10.1002/rog.20023, 2013.
- 850 Yde, J. C., Knudsen, N. T., Steffensen, J. P., Carrivick, J. L., Hasholt, B., Ingeman-Nielsen, T.,
851 Kronborg, C., Larsen, N. K., Mernild, S. H., Oerter, H., Roberts, D. H., and Russell, A. J.:
852 Stable oxygen isotope variability in two contrasting glacier river catchments in Greenland,
853 *Hydrology and Earth System Sciences*, 20, 1197–1210, 10.5194/hess-20-1197-2016, 2016.
- 854 Yong, B., Wang, C.-Y., Chen, J., Chen, J., Barry, D. A., Wang, T., and Li, L.: Missing water
855 from the Qiangtang Basin on the Tibetan Plateau, *Geology*, 49, 867–872, 10.1130/g48561.1,
856 2021.
- 857 Yoshimura, K., Kanamitsu, M., Noone, D., and Oki, T.: Historical isotope simulation using
858 Reanalysis atmospheric data, *Journal of Geophysical Research*, 113,
859 10.1029/2008jd010074, 2008.
- 860 Zhang, F., Zhang, H. B., Hagen, S. C., Ye, M., Wang, D. B., Gui, D. W., Zeng, C., Tian, L. D.,
861 and Liu, J. S.: Snow cover and runoff modelling in a high mountain catchment with scarce
862 data: effects of temperature and precipitation parameters, *Hydrol. Process.*, 29, 52–65,
863 <https://doi.org/10.1002/hyp.10125>, 2015.
- 864 Zhang, Z., Chen, X., Cheng, Q., and Soulsby, C.: Storage dynamics, hydrological connectivity
865 and flux ages in a karst catchment: conceptual modelling using stable isotopes, *Hydrology*



866 and Earth System Sciences, 23, 51-71, 10.5194/hess-23-51-2019, 2019.
867



868 **List of Tables**

869

870 **Table 1.** Summary of precipitation and stream water samples in the YTR and KR catchments.

Catchment (Station)	Year	Sampling dates (weekly)	Precipitation sample number	Stream sample number
YTR (Nuxia)		14/Mar to 23/Oct	86	34
YTR (Yangcun)	2005	17/Mar to 05/ Oct	59	30
YTR (Nugesha)		14/Mar to 22/ Oct	45	25
YTR (Lazi)		06/ Jun to 22/Sep	42	22
	2006	04/Jun to 11/Nov	24	31
	2007	23/Apr to 09/ Oct	39	25
KR (Wengguo)	2010	05/May to 18/ Oct	63	23
	2011	28/Mar to 06/Nov	69	32
	2012	16/ Jun to 22/ Sep	42	14

871

872



873 **Table 2.** Calibrated parameters of the THREW-T model

Symbol	Unit	Physical descriptions	Value range
nt	-	Manning roughness coefficient for hillslope	0-0.2
WM	cm	Tension water storage capacity, used in Xinanjiang model to calculate saturation area	0-10
B	-	Shape coefficient used in Xinanjiang model to calculate saturation area	0-1
KK_A	-	Coefficient to calculate subsurface runoff in $Rg=KKD \cdot S \cdot K^S_S \cdot (y_s/Z)^{KK_A}$, where S is the topographic slope, K^S_S is the saturated hydraulic conductivity, y_s is the depth of saturated groundwater, Z is the total soil depth	0-6
KKD	-	See description for KK_A	0-0.5
T_0	°C	Temperature threshold above which snow and glacier melt	-5-5
DDF_N	mm/°C/day	Degree day factor for snowmelt	0-10
DDF_G	mm/°C/day	Degree day factor for glacier melt	0-10
CI	-	Coefficient to calculate the runoff concentration process using Muskingum method: $O_2=C_1 \cdot I_1+C_2 \cdot I_2+C_3 \cdot O_1+C_4 \cdot Q_{lat}$, where I_1 and O_1 is the inflow and outflow at prior step, I_2 and O_2 is the inflow and outflow at current step, Q_{lat} is lateral flow of the river channel, $C_3=I-C_1-C_2$, $C_4=C_1+C_2$	0-1
$C2$	-	See description for CI	0-1

874



75 **Table 3.** Descriptions of water sampling scenarios in the three numerical experiments. $\delta^{18}\text{O}_{\text{GM}}$ is the assumed glacier meltwater
 76 isotope signature and $\overline{\delta^{18}\text{O}_{\text{PR}}}$ refers to the long term mean isotope signature of precipitation.

Experiment	Scenarios	Isotope data conditions
Benchmark model running in the YTR basin	BM_YTR	Using assumed glacier meltwater isotope as: $\delta^{18}\text{O}_{\text{GM}} = \overline{\delta^{18}\text{O}_{\text{PR}}} - 5\%$ Using IsoGSM outputs that were corrected by sample measurements of precipitation isotope from four sampling sites Using all available stream water samples in the study period to calibrate the model
Benchmark model running in the KR catchment	BM_KR	Using all available stream water samples in the study period to calibrate the model
Experiment 1: Estimate of glacier meltwater isotope	G_Δ1	Assuming glacier meltwater isotope as: $\delta^{18}\text{O}_{\text{GM}} = \overline{\delta^{18}\text{O}_{\text{PR}}} - 1\%$
	G_Δ3	Assuming glacier meltwater isotope as: $\delta^{18}\text{O}_{\text{GM}} = \overline{\delta^{18}\text{O}_{\text{PR}}} - 3\%$
	G_Δ7	Assuming glacier meltwater isotope as: $\delta^{18}\text{O}_{\text{GM}} = \overline{\delta^{18}\text{O}_{\text{PR}}} - 7\%$
	G_Δ9	Assuming glacier meltwater isotope as: $\delta^{18}\text{O}_{\text{GM}} = \overline{\delta^{18}\text{O}_{\text{PR}}} - 9\%$
Experiment 2: Site sampling data of precipitation isotope	P_1station	Using IsoGSM outputs corrected by measurements of precipitation isotope collected at one station (Nuxia) in YTR
	P_2stationNY	Using IsoGSM outputs corrected by measurements of precipitation isotope collected at two stations (Nuxia and Yangcun) in YTR
	P_2stationNL	Using IsoGSM outputs corrected by measurements of precipitation isotope collected at two stations (Nuxia and Lazi) in YTR
Experiment 3: Stream water sampling strategy for model evaluation	RT_YTR_BM	Sampling strategy: time series sampling; Sampling timing: wet season; Sampling frequency: weekly; Duration of sampling period: 1 year; Number of sampling site: 1 station
	RT_YTR_WholeYear	Same to RT_YTR_BM, but with the sampling timing as the whole study years
	RT_YTR_Monthly	Same to RT_YTR_BM, but with the sampling frequency as monthly
	RT_YTR_2year	Same to RT_YTR_BM, but with the duration of sampling period as only 2 years
	RT_YTR_3year	Same to RT_YTR_BM, but with the duration of sampling period as only 3 years
	RT_YTR_2station	Same to RT_YTR_BM, but with the number of sampling site as 2 stations
	RT_YTR_4station	Same to RT_YTR_BM, but with the number of sampling site as 4 stations
	RS_YTR_Main	Sampling strategy: spatially distributed sampling in a single field campaign; Location of sampling site: along the main stream
	RS_YTR_Tributary	Same to RS_YTR_Main, but using stream water samples from additional sites along the tributaries
	RT_KR_1year	Sampling strategy: time series sampling; Duration of sampling period: 1 year
	RT_KR_2year	Same to RT_KR_1year, but with the duration of sampling period as 2 years
RT_KR_3year	Same to RT_KR_1year, but with the duration of sampling period as 3 years	
RT_KR_4year	Same to RT_KR_1year, but with the duration of sampling period as 4 years	
RT_KR_5year	Same to RT_KR_1year, but with the duration of sampling period as 5 years	

77
78



879 **Table 4.** Contributions (%) of runoff components in the YTR basin and KR catchment
 880 estimated by different calibration variants in the benchmark scenario.

Runoff Component	YTR basin		KR catchment	
	Bi-objective calibration*	Tri-objective calibration	Bi-objective calibration	Tri-objective calibration
Rainfall	62.8 (± 6.5)	70.7 (± 2.5)	46.4 (± 5.0)	43.9 (± 1.4)
Snowmelt	10.8 (± 1.1)	12.2 (± 0.4)	22.6 (± 2.4)	21.4 (± 0.7)
Glacier melt	26.4 (± 7.5)	17.1 (± 2.9)	31.0 (± 7.4)	34.6 (± 2.0)
Surface runoff	52.1 (± 0.5)	44.7 (± 6.7)	62.0 (± 10.9)	75.1 (± 3.3)
Subsurface runoff	47.9 (± 10.5)	55.3 (± 6.7)	38.0 (± 10.5)	24.9 (± 3.3)

881 *: Values in brackets refer to the standard deviation of the contribution of runoff component produced
 882 by the behavioral parameter sets.

883



884 **Table 5.** Benchmark parameter set and corresponding model behavior that are used to produce
 885 stream water $\delta^{18}\text{O}$ data for model calibration in experiment 3 in YTR basin.

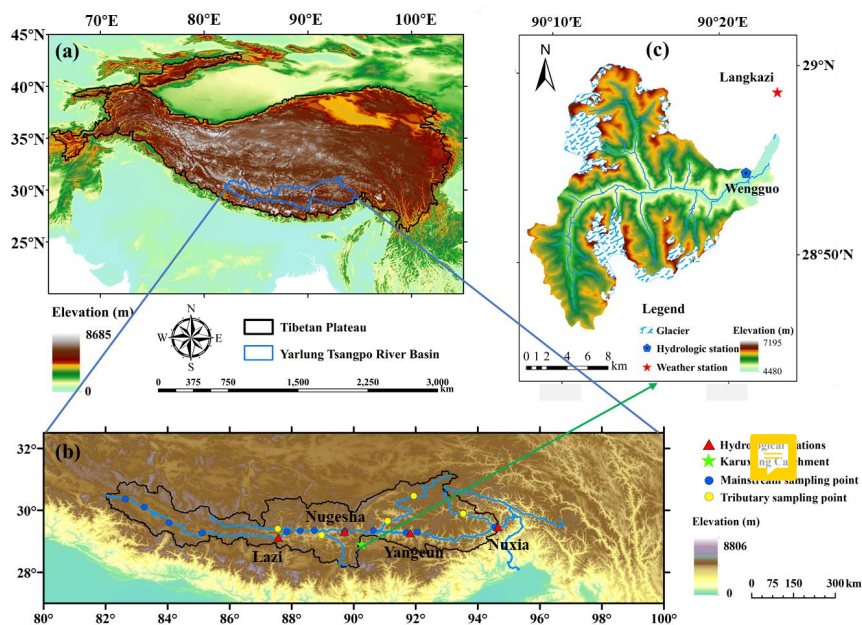
Parameter value		Model behavior	
<i>nt</i>	0.09	NSE _{dis} (Nuxia,calibration)	0.87
<i>WM</i>	0.92	NSE _{dis} (Nuxia,validation)	0.80
<i>B</i>	0.62	RMSE _{SCA} (calibration)	0.08
<i>KKA</i>	3.22	RMSE _{SCA} (validation)	0.12
<i>KKD</i>	0.14	NSE _{iso}	0.58
<i>T₀</i>	1.59	NSE _{dis} (Yangcun)	0.85
<i>DDF_N</i>	8.04	NSE _{dis} (Nugesha)	0.76
<i>DDF_G</i>	8.28	Contribution of rainfall	70%
<i>C1</i>	0.0004	Contribution of snowmelt	12%
<i>C2</i>	0.075	Contribution of glacier melt	18%
		Contribution of baseflow	56%

886



887 **List of Figures**

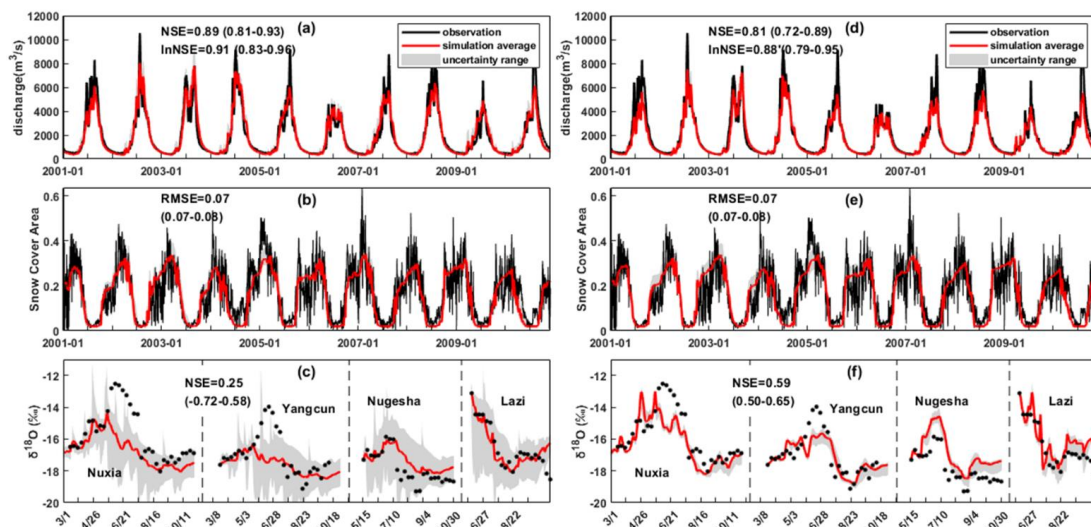
888



889

890 **Figure 1.** Locations and topography of the (a) Tibetan Plateau, (b) Yarlung Tsangpo river
891 basin and (c) Karuxung catchment. Triangles in figure b refer to hydrometric stations and
892 sampling sites for precipitation and stream water isotope. Dots in figure b refer to assumed
893 stream water sampling locations in RD_YTR scenarios.

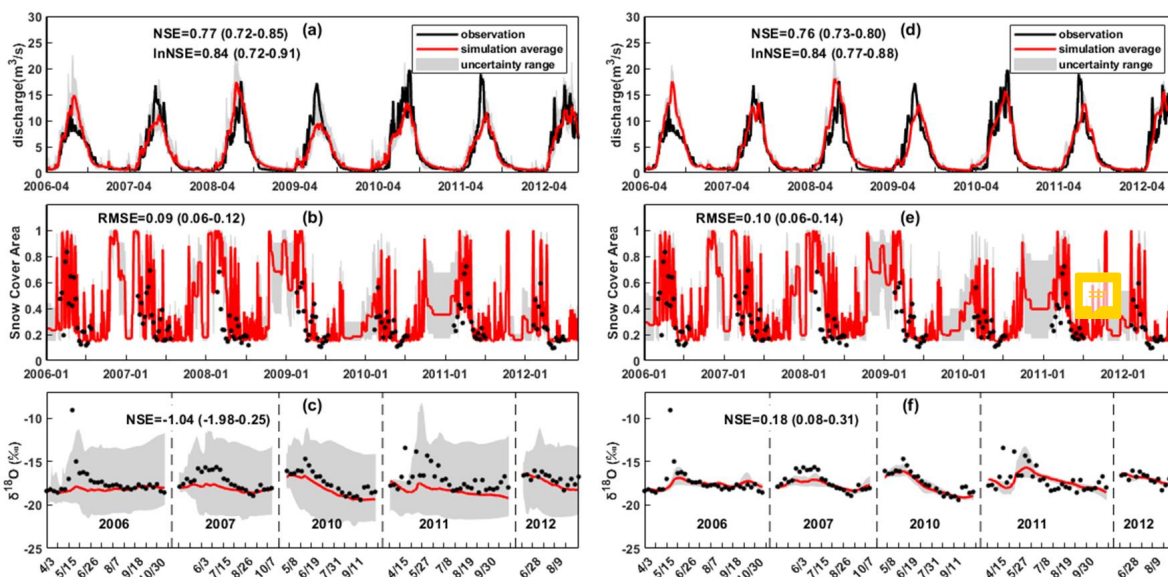
894



895

896 **Figure 2.** Uncertainty ranges and metrics values of the simulated discharge (Nuxia station),
897 SCA, and stream $\delta^{18}\text{O}$ (at four stations during 2001–2009) in the YTR basin, that were produced by
898 the behavioral parameter sets of a bi-objective calibration (a-c) and a tri-objective (d-f)
899 calibration in the benchmark model running.

900

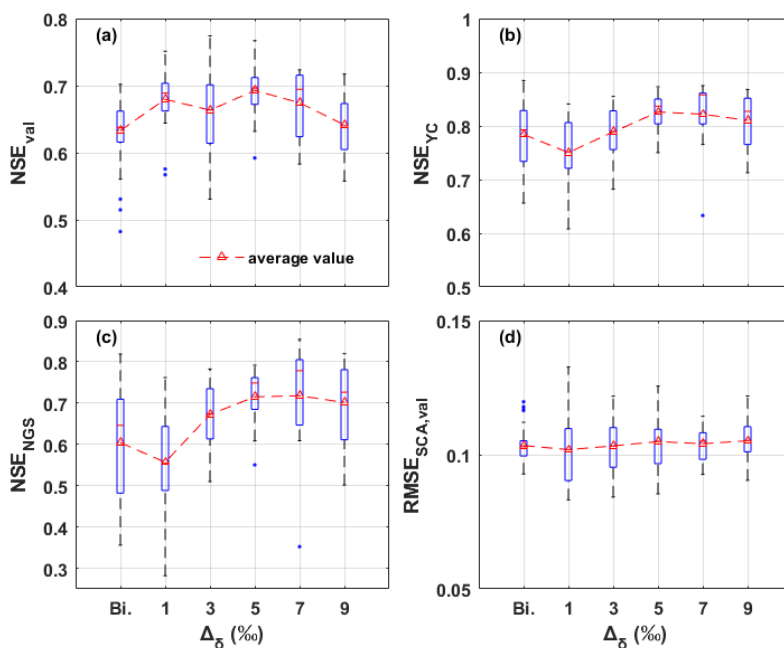


901

902 **Figure 3.** Uncertainty ranges and metrics values of the simulated discharge, SCA, and stream
903 $\delta^{18}\text{O}$ in the KR catchment produced by the behavioral parameter sets of a bi-objective
904 calibration (a-c) and a tri-objective (d-f) calibration in the benchmark model running.

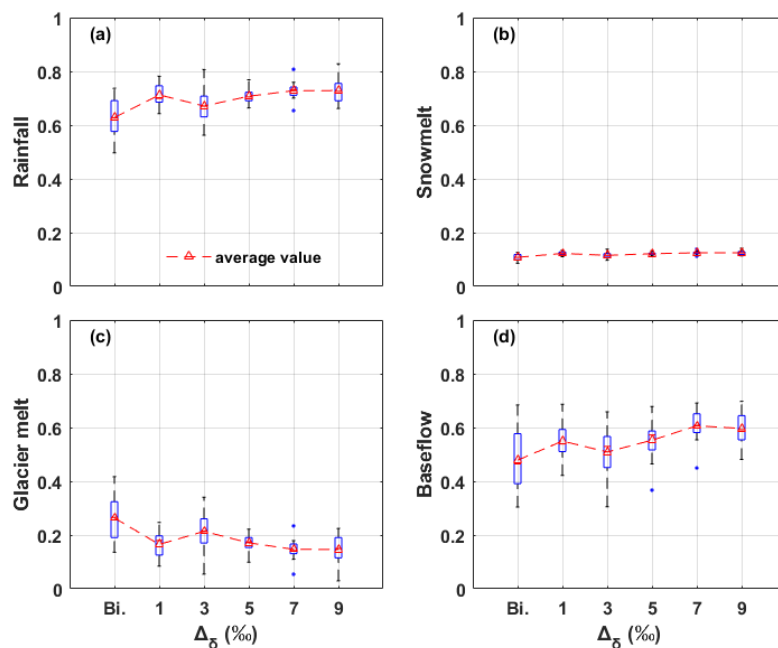


905

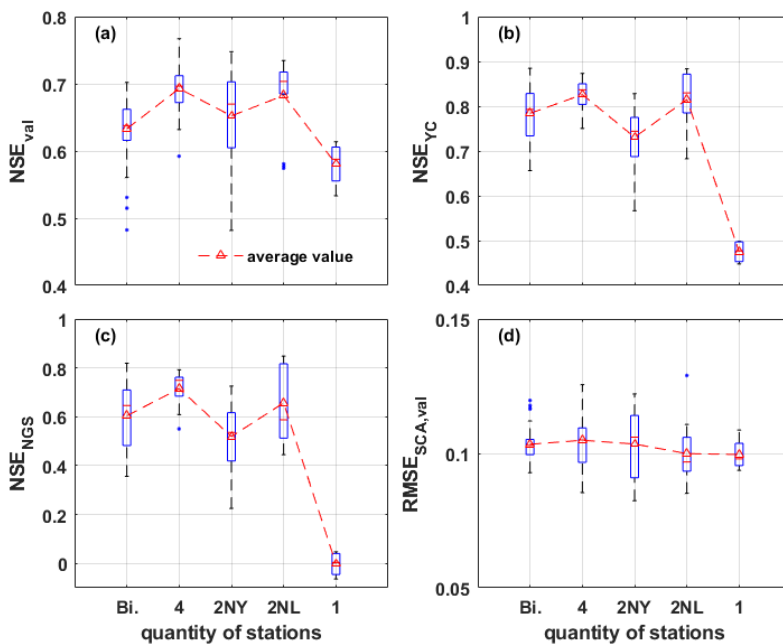


906

907 **Figure 4.** Model performances in simulating discharge and SCA in the YTR basin in validation
908 period/station produced by the behavioral parameter sets of scenarios using different glacier
909 meltwater isotope inputs (experiment 1). Subplot (a) and (d) are the performances for Nuxia
910 streamflow and SCA simulation in validation period, respectively. Subplot (b) and (c) are the
911 performances for streamflow simulation in internal stations Yangcun and Nugesha, respectively.
912



913
914 **Figure 5.** Runoff component contributions in the YTR basin estimated by the behavioral
915 parameter sets of scenarios in experiment 1.
916

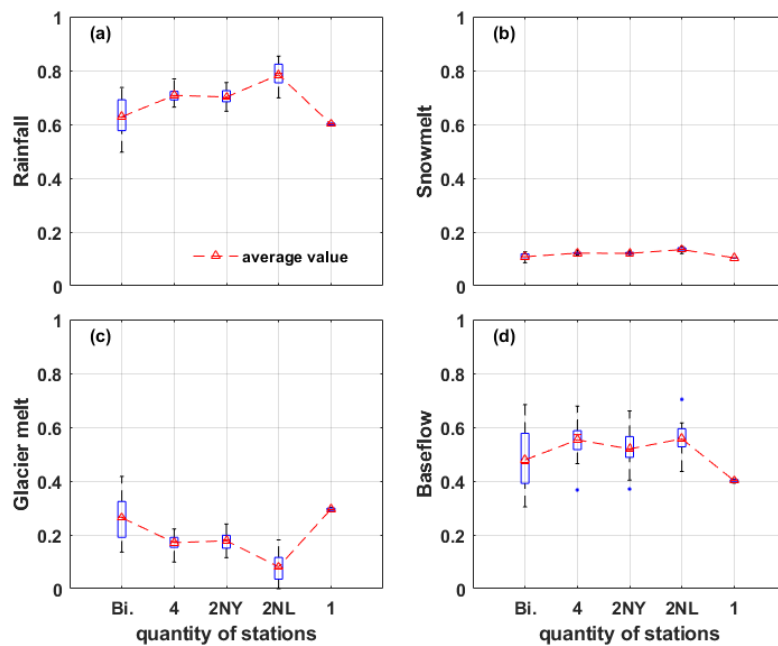


917

918 **Figure 6.** Model performances in simulating discharge and SCA validation period/station in
919 YTR basin produced by the behavioral parameter sets of scenarios using precipitation isotope
920 measurements from different sampling sites (experiment 2). Subplot (a) and (d) are the
921 performances for Nuxia streamflow and SCA simulation in validation period, respectively.
922 Subplot (b) and (c) are the performances for streamflow simulation in internal stations Yangcun
923 and Nugesha, respectively.



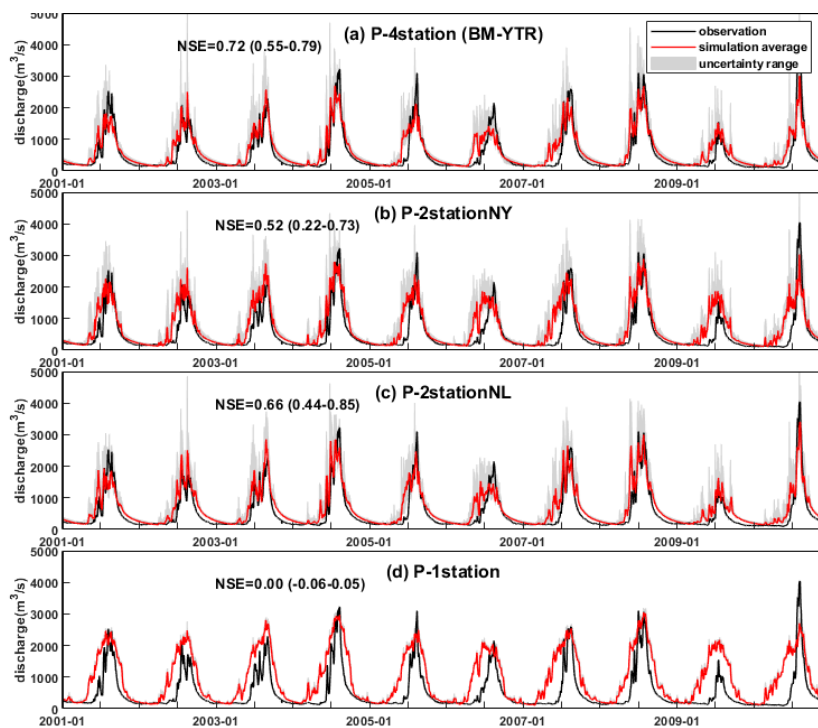
924



925

926 **Figure 7.** Runoff component contributions in the YTR basin estimated by the behavioral
927 parameter sets of scenarios in experiment 2.

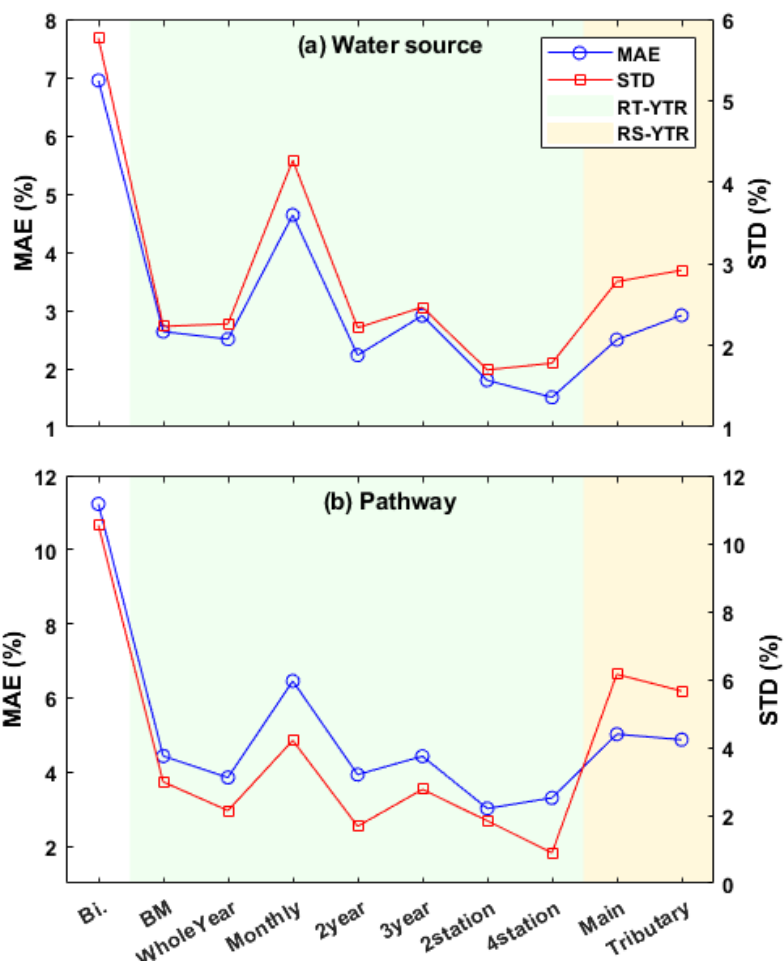
928



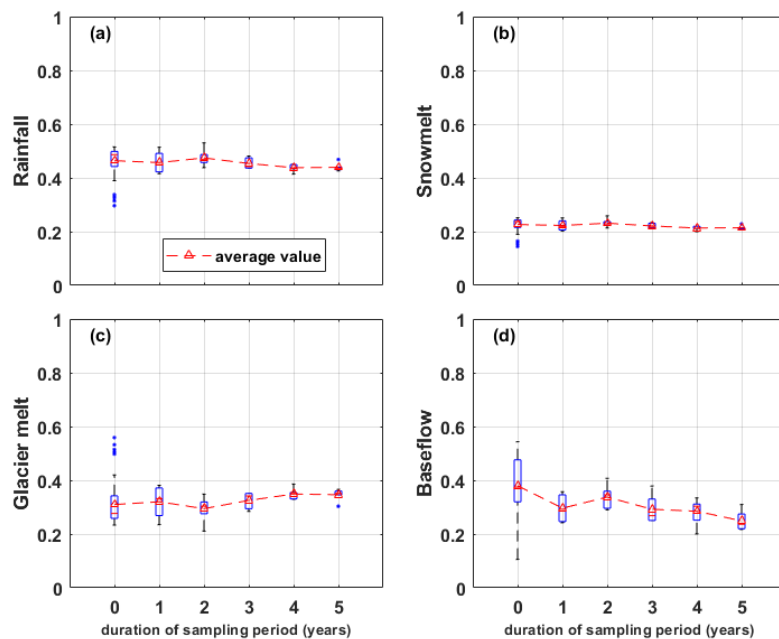
929

930 **Figure 8.** Uncertainty range and metrics values of simulated discharge at Nugesha station
931 produced by the behavioral parameter sets of each scenario in experiment 2.

932

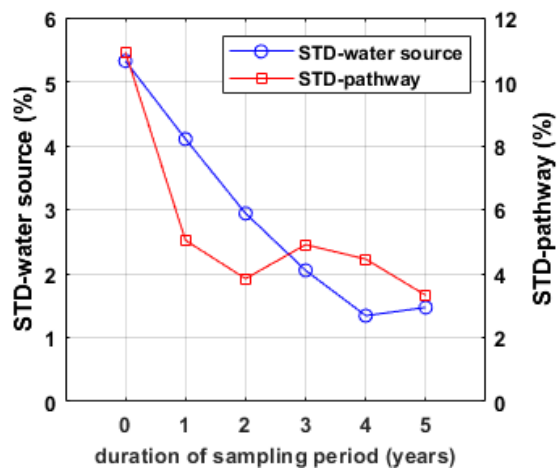


933
934 **Figure 9.** Accuracy and uncertainty metrics of estimated CRCs in the YTR basin derived from
935 the different stream water sampling strategies (experiment 3). (a) for CRCs quantified under
936 the definition of water source and (b) for CRCs quantified under the definition of runoff
937 pathway.
938



939

940 **Figure 10.** Uncertainties of the contributions of (a) rainfall, (b) snowmelt, (c) glacier melt and
941 (d) baseflow in the KR catchment, estimated by scenarios with different durations of
942 sampling period (experiment 3).
943



944

945 **Figure 11.** Uncertainty metrics of estimated CRCs in the KR catchment estimated by
946 scenarios with different durations of sampling period.

947